

Economic valuation of subsurface water contributions to watershed ecosystem services using a fully-integrated groundwater–surface water model

Tariq Aziz^{1,2,*}, Steven K. Frey^{1,3}, David R. Lapen⁴, Susan Preston⁵, Hazen A. J. Russell⁶, Omar Khader^{1,7}, Andre R. Erler¹, Edward A. Sudicky^{1,3}

¹Aquanty, 600 Weber St. N., Unit B, Waterloo, ON, N2V 1K4, Canada

²Ecohydrology Research Group, Water Institute and Department of Earth and Environmental Sciences, University of Waterloo, Waterloo, N2L 3G1, ON, Canada

³Department of Earth and Environmental Sciences, University of Waterloo, Waterloo, N2L 3G1, ON, Canada

⁴Agriculture and Agri-Food Canada, Ottawa Research and Development Centre, Ottawa, Ontario, Canada

⁵Environment and Climate Change Canada, Ottawa, Ontario, Canada

⁶Geological Survey of Canada, 601 Booth St., Ottawa, ON, K1A 0E8, Canada

⁷Department of Water and Water Structural Engineering, Zagazig University, AlSharqia, Egypt

*Correspondence to: Tariq Aziz (taziz@aquanty.com)

Abstract. Water is essential for all ecosystem services, yet a comprehensive assessment and economic valuation of total (overall) water contributions to ecosystem services production using a fully-integrated groundwater-surface water model has never been attempted. Quantification of the many ecosystem services impacted by water demands an analytical approach that implicitly characterizes both subsurface and surface water resources; however, incorporating subsurface water into ecosystem services evaluation is a recognized scientific challenge. In this study, a fully-integrated groundwater–surface water model—HydroGeoSphere (HGS)— is used to capture changes in subsurface water, surface water, and transpiration (green water use), and along with an economic valuation approach, forms the basis of an ecosystem services assessment for an 18-year period (2000-2017) in the 3830 km² South Nation Watershed (SNW), a mixed-use but a predominantly agricultural watershed in eastern Ontario, Canada. Using green water volumes generated by HGS and ecosystem services values as inputs, the marginal productivity of water is calculated to be \$0.26 per m³ (in 2022 Canadian dollars). Results show maximum green water values during the driest years, with the extreme drought of 2012 being the highest at \$424.7 million. In contrast, the green water value in wetter years was as low as \$245.9 million, while the 18-year average was \$338.83 million. Because subsurface water is the sole contributor to the green water supply it plays a critical role in sustaining ecosystem services during drought conditions. This study provides new insight into the economic contributions of subsurface water and its role in sustaining ecosystem services during droughts, and puts forth improved methodology for watershed-based management and valuation of ecosystem services.

1 Introduction

The role of subsurface water (including groundwater and soil moisture) in socio-economic development is widely acknowledged (Foster and Chilton, 2003); however, its ecological contributions are undervalued (Yang and Liu, 2020), despite being fundamental to the control of terrestrial ecological processes (Qiu et al., 2019). Subsurface water

36 supports numerous ecosystem services that range from provisioning to regulating, supporting, and cultural services
37 (Griebler and Avramov, 2015). While infiltration is a driver for subsurface water recharge, subsurface water discharge
38 and vegetation uptake are, in-turn, key fluxes for supporting terrestrial ecosystems (e.g., wetlands, forests, crops, etc.)
39 (Griebler and Avramov, 2015). Subsurface water can provide a buffer against weather stressors on vegetation and
40 aquatic ecosystems and helps to maintain key processes that underpin ecosystem services (Qiu et al., 2019). To date,
41 most ecosystem services research has focused on aboveground factors and processes (e.g., land use change), and very
42 little focus has been given to subsurface water and its influence on terrestrial ecosystem services (Richardson and
43 Kumar, 2017; Qiu et al., 2019). While some previous research (e.g., Booth et al., 2016; Li et al., 2014) has attempted
44 to link subsurface water with land cover, it typically reflects field scale, static environmental conditions (Qiu et al.,
45 2019). Given the challenges with mapping subsurface water resources, the contribution of subsurface water towards
46 terrestrial ecosystem services is not typically quantified, and the economic value of subsurface water contribution to
47 terrestrial ecosystem services is therefore not assessed.

48 While hydrologic ecosystem services studies are common in the literature (Ochoa and Urbina-Cardona, 2017),
49 groundwater-focused ecosystem services assessments are rare. However, groundwater can be an important regulator
50 of watershed hydrologic behaviour and ecosystem health, especially in regions with a shallow water table, such as the
51 Laurentian Great Lakes Region (Neff et al., 2005; Kornelsen and Coulibaly, 2014). In such areas, groundwater acts
52 as a source of soil water (Chen and Hu, 2004). The importance of groundwater has been noted by Griebler and
53 Avramov (2015) in their review of groundwater ecosystem services, where they highlight the direct role it plays in
54 supplying different types of ecosystem services (Millenium Ecosystem Assessment (MEA), 2005); and they stress the
55 need for a better quantitative understanding of groundwater processes in order to protect and manage groundwater and
56 its ecosystem services. Furthermore, Mammola et al. (2019) emphasize that subterranean ecosystems are largely being
57 overlooked in conservation policies. Based on a preliminary assessment of all the regions around the world where
58 groundwater plays a critical role in ecosystem services, and considering that approximately 43 % of consumptive
59 irrigation is sourced from groundwater (Siebert et al., 2010), the lack of focus on subsurface water ecosystem services
60 is not due to lack of need, rather the lack of use of suitable tools to conduct the required analysis.

61 Hydrological models can efficiently and accurately quantify water storages and fluxes over large spatial scales. With
62 groundwater ecosystem services' increasing role in policy-making (Honeck et al., 2021) and sustainable groundwater
63 resources management, new tools are required for their mapping. At present, common modeling tools available for

64 ecosystem services mapping include relatively simple matrix models (i.e., Decsi et al., 2022), and more complex
65 models such as ARTificial Intelligence for Environment & Sustainability (ARIES) (Villa et al., 2021), Co\$ting Nature
66 (Mulligan, 2015), Envision (Bolte, 2022), and Integrated Valuation of Ecosystem Services and Tradeoffs (InVEST)
67 (Natural Capital Project, 2022), with InVEST being by far the most prominent in the scientific literature (Ochoa and
68 Urbina-Cardona, 2017). However, ecosystem services specific models, such as the InVEST Water Yield Model, have
69 limited capability to simulate all relevant hydrological processes (Redhead et al. 2016), because their hydrologic tools
70 typically focus on one water compartment and/or are simplified to the point where hydrologically mediated ecosystem
71 services cannot be fully characterized (Dennedy-Frank et al., 2016; Vigerstol and Aukema, 2011). Complete
72 characterization of spatially and temporally varying water storages and fluxes that govern ecosystem services over
73 large spatial scales requires more sophisticated, process-based hydrological models (Sun et al., 2017). Hence, models
74 like SWAT (Arnold et al., 1998) and the Variable Infiltration Capacity (VIC) model (Liang et al., 1994) have been
75 used for hydrologic ecosystem services assessment, however even these models are limited in their ability to simulate
76 complex subsurface water movement and water exchanges between the surface and subsurface. Within the hydrologic
77 modeling community, it is acknowledged that structurally complex, fully-integrated subsurface–surface water models
78 are the current state-of-the-art for capturing the interplay between subsurface and surface water systems across a wide
79 range of spatial scales (Barthel and Banzhaf, 2016; Berg and Sudicky, 2019), however, this class of models, to best of
80 our knowledge, has not yet been applied towards ecosystem services valuation.

81 In humid climates, evapotranspiration is often the most significant component of the hydrologic cycle after
82 precipitation, and must be carefully considered when modelling near surface hydrologic processes. Evapotranspiration
83 is a fraction of rainfall that eventually returns to the atmosphere through evaporation and transpiration (Jin et al., 2017;
84 Condon et al., 2020), which represent large fluxes of both water and energy across the land surface–atmosphere
85 boundary (Tan et al., 2021). Transpiration, a dominant flux in evapotranspiration, results from plant use of green
86 water—the water in the soil available to plants (Casagrande et al., 2021). Thus, green water, by extension, is crucial
87 for ecosystem functioning (An and Verhoeven, 2019), and supporting ecosystem services associated with healthy and
88 productive plant life (Zisopoulou et al., 2022; Schyns et al., 2019). Hence, transpiration serves as a key driver in
89 providing ecosystem services (Liu and El-Kassaby, 2017), and is a fundamental process by which to model/map
90 terrestrial ecosystem services production. For example, the degree of transpiration in an ecosystem is tied to subsurface
91 water available to plants, temperature, wind, light, and stomatal controls (Lowe et al., 2022). While specifically

92 capturing the interplay between green water and transpiration rates is complex, the generalized linkage between them
93 is nevertheless useful for valuing green water in supporting ecosystem services provided by transpiring vegetation;
94 and fully-integrated hydrological models that capture subsurface-surface water interactions, will be necessary
95 analytical tools in this regard.

96 Changes in evapotranspiration can influence water availability and ecosystem health at a watershed scale (Zhao et al.,
97 2022). Under drought conditions, subsurface water reserves can become critically important for sustaining plant
98 growth (Condon et al., 2020), and hence, mapping linkages between subsurface water and transpiration is important
99 for sustainable water and ecosystem services management (Yang et al., 2015). Fully integrated subsurface-surface
100 hydrologic models are potentially well suited for such mapping applications. A number of fully-integrated subsurface-
101 surface models have been developed, and benchmarking studies have been conducted wherein select models have
102 been described in detail, and their simulation behavior compared (Maxwell et al., 2014; Kollet et al., 2016).

103 In this study, the HydroGeoSphere (HGS) fully-integrated subsurface–surface water model (Aquanty, 2021; Brunner
104 and Simmons, 2012) is introduced as a tool for mapping hydrological fluxes and water storage fluctuations, and
105 quantifying subsurface water contributions to terrestrial ecosystem services at the watershed scale (~4000 km²). In
106 combination with a benefits transfer approach, the results from HGS modelling are extended to an economic valuation
107 of water contributions to ecosystem services. Until now, fully-integrated subsurface-surface models such as HGS have
108 not been widely demonstrated in the scientific literature as tools for modeling ecosystem services, while at the same
109 time, the economic value of subsurface water has been overlooked in ecosystem services valuation assessments.
110 Accordingly, the study improves our understanding of overall hydrologic contributions to ecosystem services.
111 Furthermore, using the HGS model outputs to support the economic valuation of subsurface water contributions to
112 transpiration, and ultimately to terrestrial ecosystem services, is also novel. Hence, this work helps to advance the
113 science of ecosystem service valuation in terms of conceptual, methodological, and quantitative understanding.
114 Results from this study are also directly relevant to the broader scientific and policymaking communities who are
115 seeking insights into the role of subsurface water in supporting societal endpoints under a wide range of different
116 climatological conditions in humid continental climates.

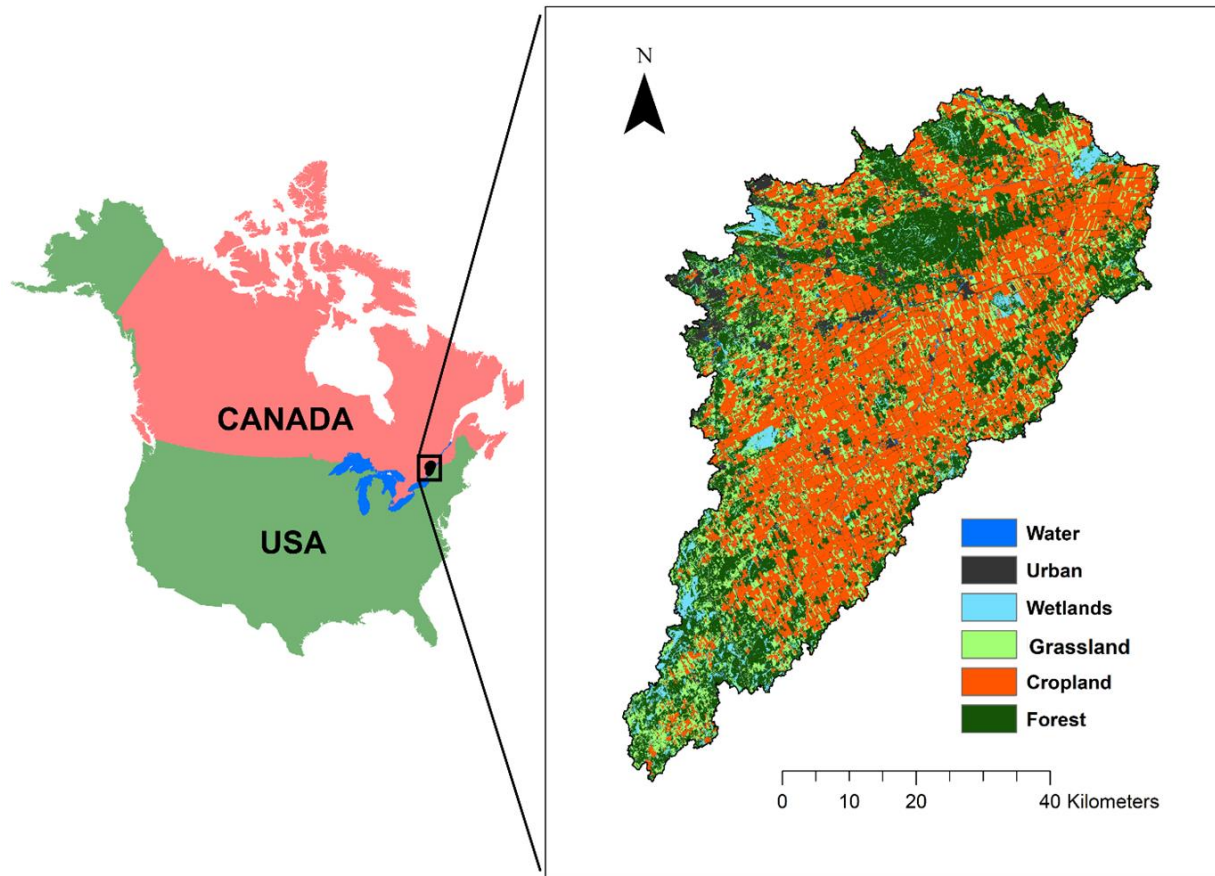
117 2 Materials and methods

118 2.1 Study area

119 This study focuses on the South Nation watershed (SNW), located in eastern Ontario, Canada, with an area of
120 approximately 3,830 km² (Fig. 1). The SNW is relatively flat, with approximately 100 m of vertical relief in the land
121 surface (Fig. A1). It is primarily an agriculture-focused watershed, with relatively low population density. The eastern
122 flank of the city of Ottawa encroaches on the Northwest corner of the watershed. The SNW surface water flow network
123 is approximately 6,489 km long and consists of 1,606 km of Strahler order 3+ (relatively large), 1,548 km of Strahler
124 order 2, and 3,335 km of Strahler order 1 (smallest) waterways (Fig. A2). Many of the low order features are either
125 manmade agricultural drainage ditches or straightened natural watercourses designed to drain the agricultural
126 landscape.

127 Soil drainage conditions across the watershed are generally imperfect, poor, or very poor (Fig. A3), with some pockets
128 are considered as well drained (Soil Landscapes of Canada Working Group, 2010). The wide extent of poorly drained
129 soils in the SNW necessitates subsurface tile drainage for crop production. Tile drainage is employed widely in the
130 watershed to enhance agricultural productivity and to facilitate cropping activities (Fig. A4). Across most of the SNW
131 the soils are primarily underlain by glacial, fluvial, and colluvial Quaternary deposits (Ontario Geological Survey,
132 2010). These sediments are composed of sand, silt, clay, gravel, and glacial till, and range in thickness from 0 m to
133 approximately 90 m across the watershed. Eight soils have been identified in the SNW (Soil Landscapes of Canada
134 Working Group, 2010), mainly composed of clay loam and sandy loam textures (Fig. A3 (a)). Localized incised
135 bedrock channels and Quaternary esker deposits (Cummings et al., 2011) are important sources of groundwater for
136 both ecological function and human/livestock supply, and most of the rural residents in the SNW rely on groundwater
137 for domestic and farm use.

138 The SNW is characterized by relatively wet temperate climate with cold winters and warm summers. The annual
139 average temperature is just over 5 C, with average summer highs reaching 26°C in July and average winter lows
140 reaching -14°C in January (https://climate.weather.gc.ca/climate_normals). Present day landcover is given in Fig. 1.

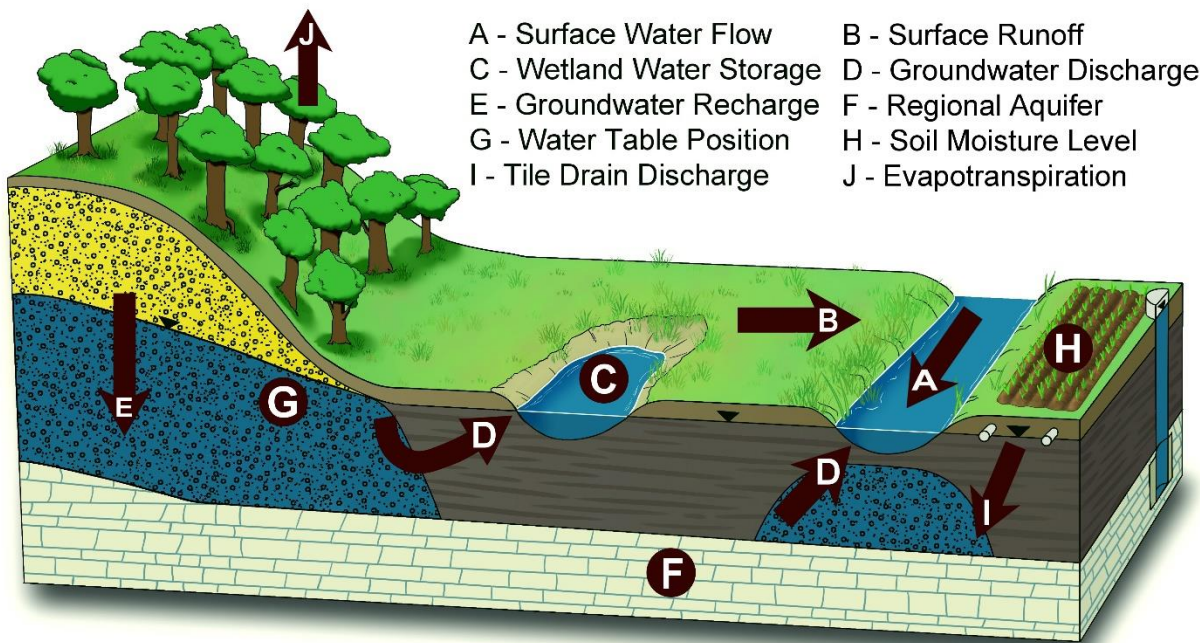


141
 142 **Figure 1: Location of the South Nation Watershed (SNW) in North America. The inset figure (right) shows the**
 143 **land use distribution across the SNW.**

144 **2.2 Water balance quantification with HydroGeoSphere (HGS)**

145 The water balance strongly influences ecosystem functions and the associated ecosystem services, as it governs both
 146 abiotic and biotic processes occurring within ecosystems (Mercado-bettín et al., 2019). Consequently, evaluating the
 147 role of water towards ecosystem services supply necessitates an analysis capable of water balance partitioning (i.e.,
 148 disaggregation of the water balance into its fundamental components such as precipitation, subsurface evaporation,
 149 transpiration, surface and subsurface storages) (Casagrande et al., 2021). As HGS is a dynamic fully-integrated
 150 subsurface–surface hydrologic model, it generates time varying simulation outputs for all components of the terrestrial
 151 hydrologic cycle (Fig. 2), thus alleviating a common limitation of ecosystem services models in that they do not
 152 account for transient behavior (Vigerstol and Aukema, 2011). HGS employs a physically based approach to simulate

153 water movement and the partitioning of precipitation input into surface runoff, streamflow, evaporation, transpiration,
154 groundwater recharge, as well as groundwater discharge into surface water bodies like rivers and lakes (Brunner and
155 Simmons, 2012). Furthermore, HGS outputs can also be generated for the entire model domain (i.e., the watershed)
156 or refined for smaller spatial scales such as subwatersheds, with the downscale limit being that of an individual finite
157 element within the finite element mesh (FEM).



158
159 **Figure 2: Key components of the terrestrial hydrological cycle captured in HGS models over a range of spatial**
160 **scales.**

161 It should be noted that the fidelity of the HGS outputs is also dependent on the model scale, with large scale models
162 generally having lower spatial resolution than small scale models as a result of computational constraints, and in some
163 cases, data constraints. For example, a model of a 766,000 km² river basin (e.g., Xu et al., 2021a) is best suited to
164 answer big picture questions (i.e., basin water balance), while a model built at similar scale to the SNW (e.g., Frey et
165 al., 2021) can be used to address questions pertaining to more localized processes (i.e., individual wetland influences,
166 groundwater recharge and discharge patterns, aquifer conditions, and soil moisture conditions). If even more localized
167 insights are required, HGS models can be constructed for field or plot scale domains (up to approximately 10 km²),
168 where questions pertaining to things such as riparian zones, soil structure, manure application, and tile drainage
169 influences on both water quantity and quality can be evaluated (Fig. 2). Thus, HGS is a scalable and robust model for

170 ecosystem services analysis across a range of different spatial scales and different levels of hydrologic process detail.
171 For the SNW, HGS is used to simulate watershed surface water outflow, transpiration (green water), subsurface water
172 storage, and land surface water storage (reflecting water held in wetlands and reservoirs) using the model construction
173 framework presented in Frey et al. (2021).

174 **2.2.1 Model construction**

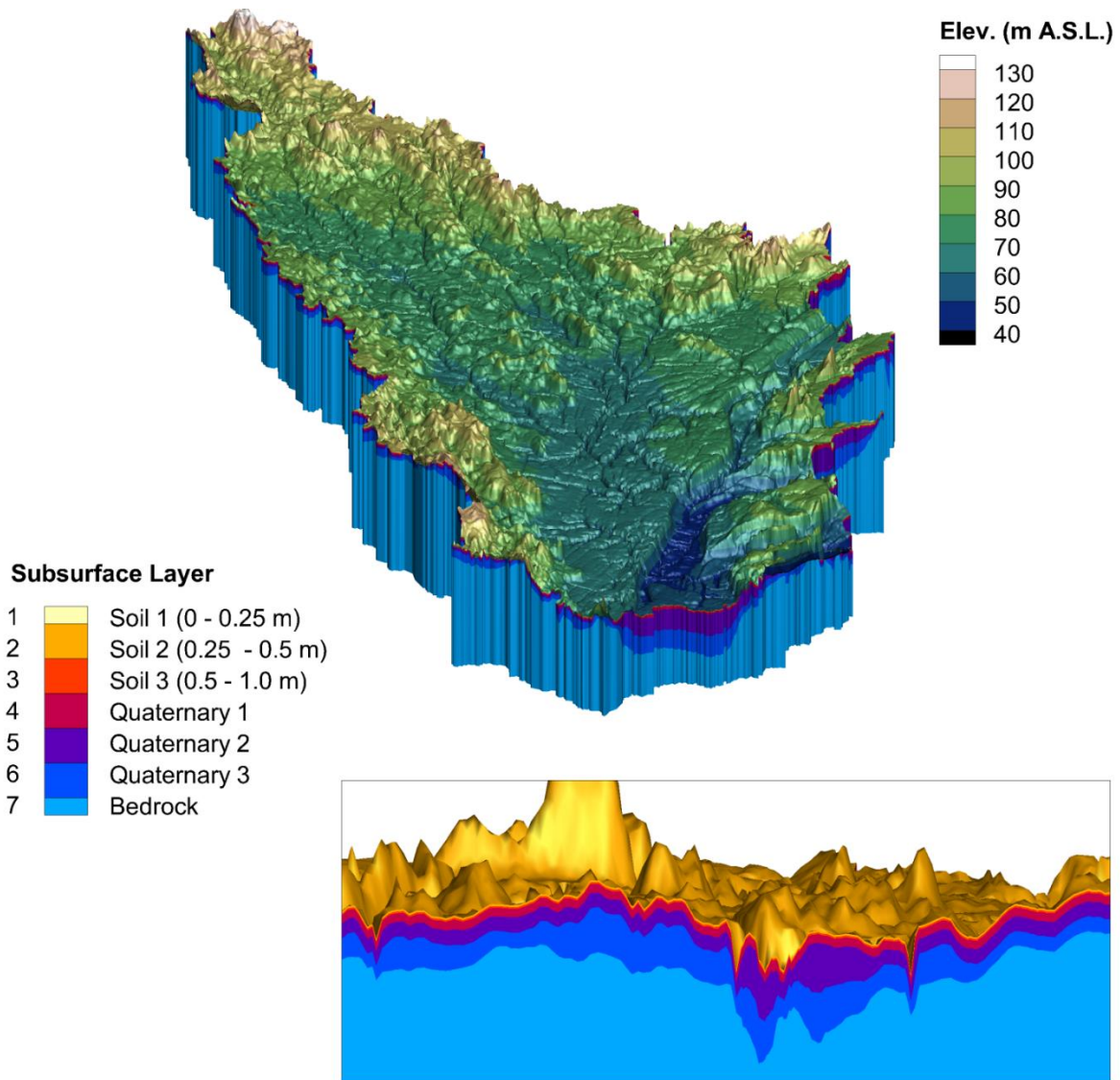
175 **2.2.1.1 Finite Element Mesh (FEM)**

176 The HGS model utilizes a 3-D unstructured FEM that extends across the full 3830 km² area of the SNW. The 1-D
177 river/stream channel features, 2-D overland flow domain (reflecting land surface topography), and 3-D subsurface
178 flow domain (reflecting hydrostratigraphy) all share the same mesh geometry, with the 1-D and 2-D domains sharing
179 common coordinates with the 3-D domain across the top surface of the model. The FEM for the SNW model resolves
180 all Strahler 2+ stream/river features as mesh discretization control lines, with element edge length maintained at 100
181 m, while away from the control lines the element edge lengths extend up to 300 m. The FEM contains layer surfaces
182 that correspond to hydrostratigraphic surfaces, with each individual layer consisting of 171,609 finite elements.
183 Accordingly, over the eight model surfaces (seven subsurface layers); the FEM contains 1,201,263 3-D finite elements.

184 **2.2.1.2 Hydrostratigraphy**

185 The seven subsurface layers represent (from the top down) three soil layers, three Quaternary hydrostratigraphic
186 layers, and one bedrock layer. The soil layers extend from 0–0.25 m, 0.25–0.5 m, and 0.5–1 m depth relative to the
187 top surface, which is defined with the Ontario Integrated Hydrology Data digital elevation model
188 (<https://geohub.lio.gov.on.ca/maps/mnrf::ontario-integrated-hydrology-oih-data/about>). The hydraulic properties for
189 the soil layers vary spatially according to the soil polygons defined in the Soil Landscapes of Canada (SLC, Soil
190 Landscapes of Canada Working Group, 2010), and are defined in two steps as follows: (1) properties extracted from
191 SLC are used in conjunction with the Rosetta pedotransfer functions (Schaap et al., 2001) to obtain estimates for
192 hydraulic conductivity, water retention and relative permeability, residual saturation, and porosity parameters, and (2)
193 hydraulic conductivity, water retention and relative permeability parameters are subsequently tuned during model
194 calibration. The three Quaternary layers are of variable thickness, where the interface surfaces represent lithology
195 contrasts derived from a simplified version of the 3-D geological model produced for the SNW by Logan et al. (2009).
196 Hydraulic properties for the Quaternary materials are assigned based on lithology. Underlying the Quaternary layers

197 is a single hydrostratigraphic layer with uniform hydraulic conductivity representative of the Phanerozoic bedrock.
198 When assembled, the model layers depict a 3-D subsurface realization of the SNW hydrostratigraphy (Fig. 3).



199
200 **Figure 3: Three-dimensional perspective of the South Nation HydroGeoSphere model, and the**
201 **hydrostratigraphic layering (inset). Note the 100x vertical exaggeration.**

202 2.2.1.3 Land surface configuration

203 The land surface in the HGS model represents land cover distribution defined by the gridded, 30 m resolution, 2017
204 Annual Crop Inventory dataset (Agriculture and Agri-Food Canada, 2022) simplified to six categories (water, urban,
205 wetland, grassland, cropland, and forest). Root depth for the cropland (1 m), forest (2.9 m), wetland (1 m), grassland
206 (2.1 m), and urban (1 m) landcovers was held static over the simulation interval. Spatially distributed leaf area index
207 (LAI) is a transient parameter defined with the 8-day composite, 500 m resolution MOD15A2H v006 data product

208 (Myneni et al., 2021). Each landcover category utilizes a unique surface roughness (Manning's n coefficient) value,
209 ranging from 0.001 (urban) to 0.03 $s/m^{1/3}$ (forest). Land cover properties, as well as subsurface hydraulic properties,
210 were mapped into the HGS model's unstructured FEM using a dominant component approach, such that when two or
211 more property classes exist within the input data set for a single finite element, the majority class is represented.

212 **2.2.1.4 Climatology**

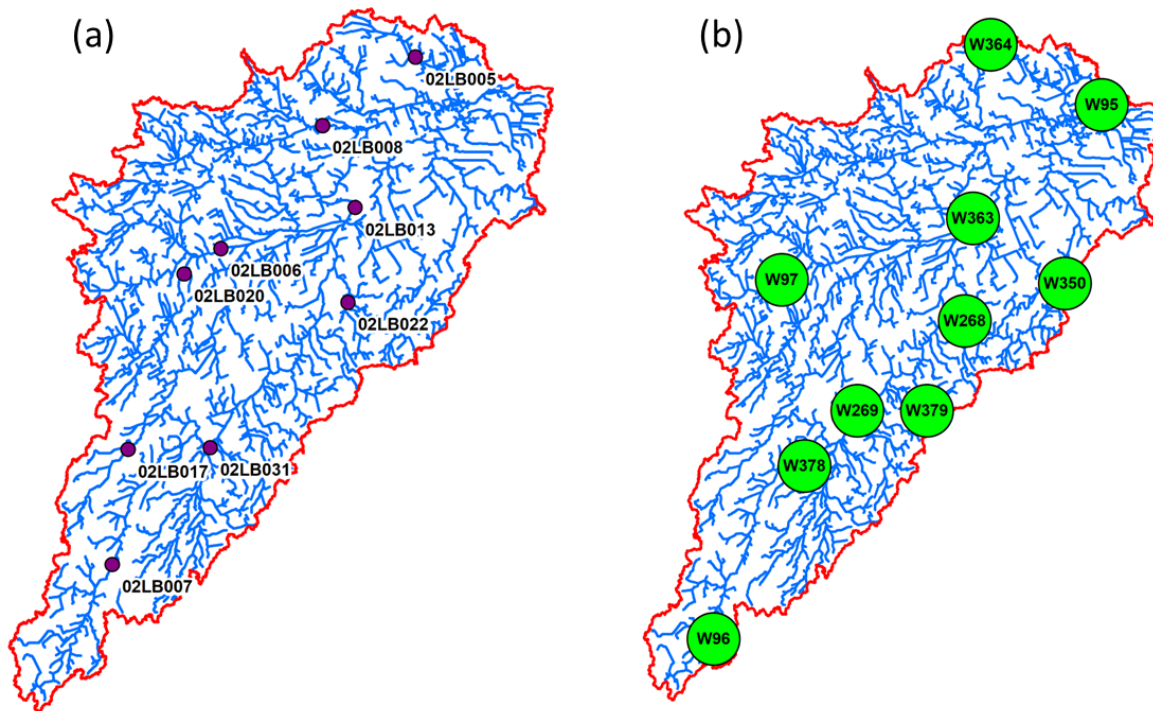
213 Time-varying and spatially distributed climate data with daily temporal resolution liquid water influx (LWF) and
214 potential evapotranspiration (PET) is used to force the HGS model for the 2000 to 2018 simulation interval. LWF is
215 derived from precipitation obtained from McKenney et al. (2011) in combination with snow water equivalent (SWE)
216 estimates from the ERA5-Land land-surface reanalysis (Muñoz-Sabater et al., 2021), where LWF is the sum of liquid
217 precipitation (rain) and snowmelt (daily changes in SWE).

218 Potential evapotranspiration primarily depends on the surface radiation budget, temperature, humidity, and near-
219 surface wind speed (Allen et al., 1998); however, of these variables, only minimum and maximum temperature are
220 readily available for the full SNW. Hence, PET forcing for the SNW model is calculated with the Hogg method (Hogg,
221 1997), which is consistent with Erler et al. (2019) and Xu et al. (2021), who both reported good agreement with the
222 observed water balance in the Great Lakes region when using the Hogg method. The Hogg method is based on the
223 FAO Penman-Monteith approach (Allen et al. 1998) with a simplification that involves the radiation budget and
224 humidity approximated as a function of daily minimum and maximum temperature, and wind speed assumed to be
225 constant.

226 **2.2.2 Model performance evaluation**

227 The SNW HGS model was run continuously for the 2000–2017 with daily temporal resolution climate forcing, and
228 simulation performance is evaluated using observed surface water flow rates and groundwater levels. The observation
229 data is derived from daily temporal resolution surface water flow monitoring conducted at nine Water Survey of
230 Canada (WSC) hydrometric stations (Figure 4a) and groundwater level data from 10 Provincial Groundwater
231 Monitoring Network wells that was collected hourly but aggregated into daily average values (Figure 4b). The Nash-
232 Sutcliffe Efficiency (NSE) and Percent Bias (Pbias) metrics (Moriasi et al., 2007) are used to evaluate surface water
233 flow simulation performance, while the coefficient of determination (R^2) and root mean square error (RMSE) is used
234 to evaluate groundwater simulation performance. It should be noted that groundwater pumping is not represented in

235 the model as it is deemed to be a very minor component of the overall water balance, and because it is extremely
236 difficult to characterize and simulate at the scale of the SNW.



237
238 **Figure 4: Distribution of (a) Water Survey of Canada surface water flow gauges, and (b) Provincial**
239 **Groundwater Monitoring Network wells across the South Nation watershed.**

240 2.3 Ecosystem services water productivity

241 The benefit transfer method is used to derive the unit values of ecosystems in the SNW. The benefit transfer method,
242 which is a widely used technique for assessing the economic value of ecosystem services, relies on secondary data
243 obtained through the implementation of various other economic valuation methods (Aziz, 2021). The benefit transfer
244 method, widely used for the economic valuation of ecosystem services, leverages existing valuation studies to estimate
245 the value of the services in different geographical contexts. The method relies on two key assumptions. First, it
246 assumes that the value of any ecosystem service (or bundle) under valuation is comparable across different regions,
247 which may not always hold true due to variations in ecological and socio-economic conditions. Additionally, the
248 methods used in the primary studies (e.g., market price, replacement cost methods) assume that market prices or the
249 costs of replacing ecosystem services accurately reflect their true value (Aziz et al., 2023). These assumptions
250 inherently limit the precision of the results, meaning the estimated values should be interpreted as approximate rather

251 than definitive. Nevertheless, these estimates provide useful insights, especially for regions like the South Nation
252 Watershed, where primary valuation studies are lacking and can guide initial policy development and resource
253 management decisions.

254 A study conducted approximately 65 km from the SNW in the Ottawa-Gatineau region, by L'Ecuyer-Sauvageau et al.
255 (2021), assembles the values for 13 ecosystem services: agricultural services, global climate regulation, air quality,
256 water provision, waste treatment, erosion control, pollination, habitat for biodiversity, natural hazard prevention, pest
257 management, nutrient cycling, landscape aesthetics, and recreational activities. These 13 ecosystem services are the
258 focus of the present analysis and their unit values have been correspondingly generated by major ecosystems using
259 market price, replacement cost, and benefit transfer methods. The unit values for ecosystem services are based on
260 similarities in ecologic and socio-economic conditions between the studied and policy sites, and converted using the
261 purchasing power parity (L'Ecuyer-Sauvageau et al., 2021). The benefit transfer method provides an approximation
262 of ecosystem service values with potential transfer errors ranging from 62% to 86% based on domestic studies (Aziz,
263 2021). In our study context, we transfer the values from the region immediately adjacent to our study region, an
264 approach that constrains the error. After adjusting these values for inflation, the value of ecosystem services in the
265 SNW is calculated using the following equation.

$$EV_t = \sum_{k=1}^n (A_k \times UV_k) * VI \quad (1)$$

267 EV_t = Value of ecosystem services for year t

268 A_k = Area of land use k

269 UV_k = Unit value of ecosystem services for land use k

270 VI = Vegetation indicator, a ratio of yearly to average net primary production (NPP) = NPP_{year}/NPP_{mean}

271 We use net primary production as an indicator to characterize the vegetation vigor (Xu et al., 2012) and to adjust the
272 values of ecosystem services over time in the SNW. The Moderate Resolution Imaging Spectroradiometer (MODIS)
273 (<https://appears.earthdatacloud.nasa.gov/>) NPP data (at 500m resolution) for the 2000 to 2017 study period is used
274 (Fig. A5). Using the ArcGIS Spatial Analyst Toolbox, yearly mean NPP values are calculated (Table 2). The average
275 ecosystem services water productivity is then calculated using ecosystem services values and productive green water
276 volumes (i.e., transpiration) in equation 2:

$$V_{wt} = (EV_t)/(X_{wt}) \quad (2)$$

278 V_{wt} is the average product of water (\$ per m³), X_{wt} is the total volume of water transpired (or volume of green water
279 used for transpiration) in a year 't'.

280 **2.4 Valuation of subsurface water contribution towards ecosystem services supply**

281 A water production function is developed using economic values of the supply of the 13 watershed ecosystem services
282 over the 18-year study period and corresponding volumes of green water used by plants for transpiration. Because
283 ecosystem services value is proportional to vegetative biomass production (Costanza et al., 1998), the values are
284 modified over time using relative changes in ecosystem vegetative biomass in the watershed (Xu and Xiao, 2022).
285 The slope of the production function represents the ecosystem services marginal water productivity (MP_w). HGS
286 model outputs capture the volume of subsurface water contributing to transpiration. Using transpired water volume
287 and MP_w , the economic value of green water is calculated (Eq.3).

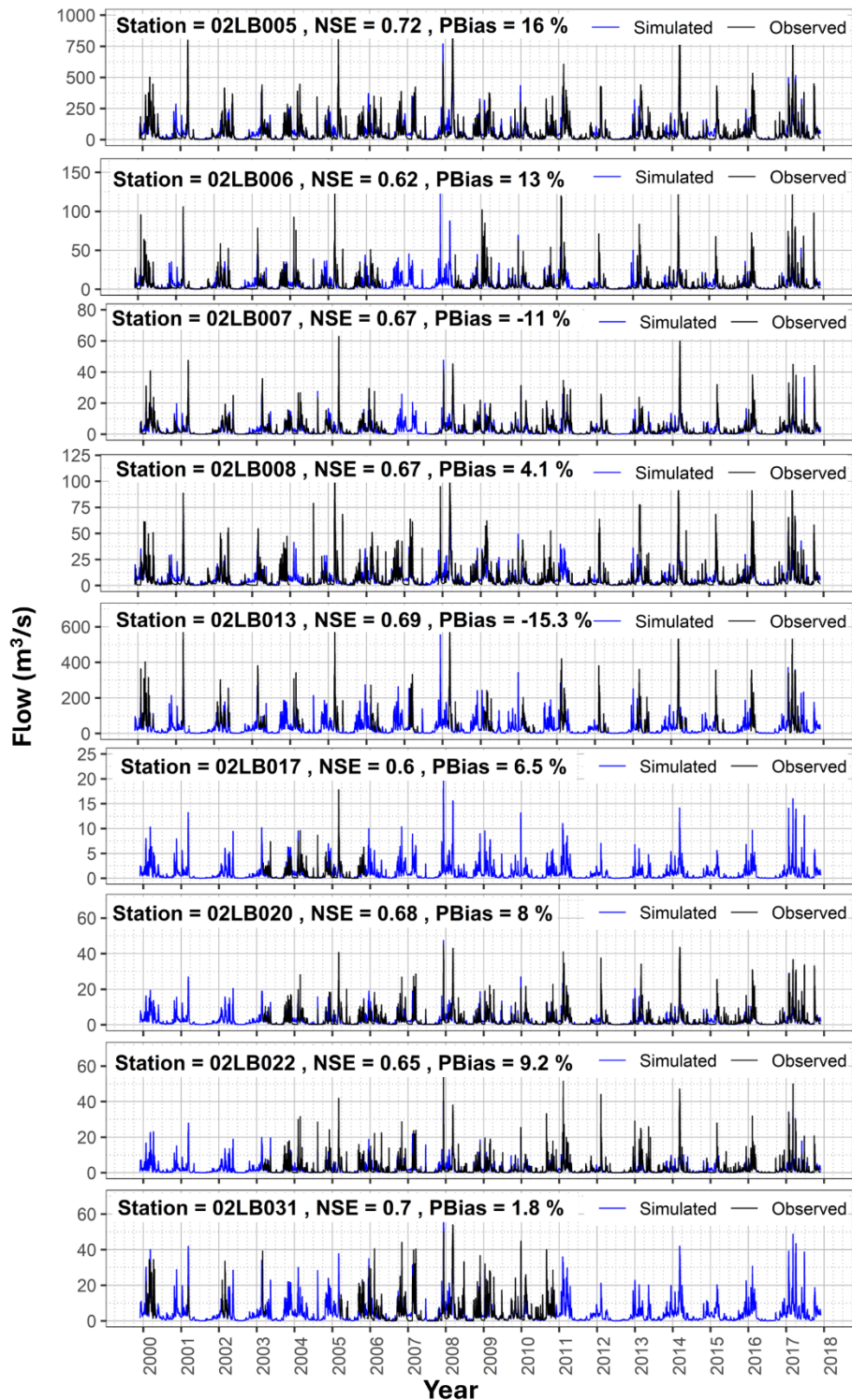
$$288 \quad V_t = X_{wt} * MP_w \quad (3)$$

289 Where V_t is the value of subsurface water used towards ecosystem services supply, X_{wt} is the volume of subsurface
290 water transpired or productive green water volume in year ‘t’, and MP_w is the marginal productivity of water.

291 **3 Results**

292 **3.1 HGS outputs**

293 For the 2000 to 2017 simulation interval, the HGS model reproduces surface water flow rates at the nine WSC
294 hydrometric stations across the SNW with good accuracy per the interpretation guidance provided by Moriasi et al.
295 (2007). Based on daily evaluation frequency, NSE at the individual gauge stations ranges from 0.59 to 0.70, with a
296 mean of 0.66; while PBias ranges from -17.4 % to 17.1 %, with a mean of 3.9 % (Fig. 5). Groundwater levels were
297 also reproduced across the SNW with reasonable accuracy for the 2000 to 2017 interval. The R^2 between simulated
298 and observed water levels in the 10 observation wells is 0.98, with the simulated values having a mean value 2.8 m
299 higher than the observed values. Groundwater simulation performance at the individual wells is presented in Table 1.
300 HGS outputs (Fig. 6) also include total watershed surface water outflow, ET_a rates (based on subsurface transpiration
301 and evaporation, surface evaporation and canopy evaporation), subsurface water storage (groundwater storage plus
302 soil moisture storage) and land surface water storage. During the simulation period, transpiration accounts for a
303 substantial proportion of ET_a , ranging from 45% to 65% (Table A1). Consequently, it emerges as the dominant process
304 contributing to the overall ET_a . As evident in Fig. 6, water storage volumes fluctuate over inter- and intra-annual time
305 frames, with the most notable decline in storage aligned closely with the drought in 2012.



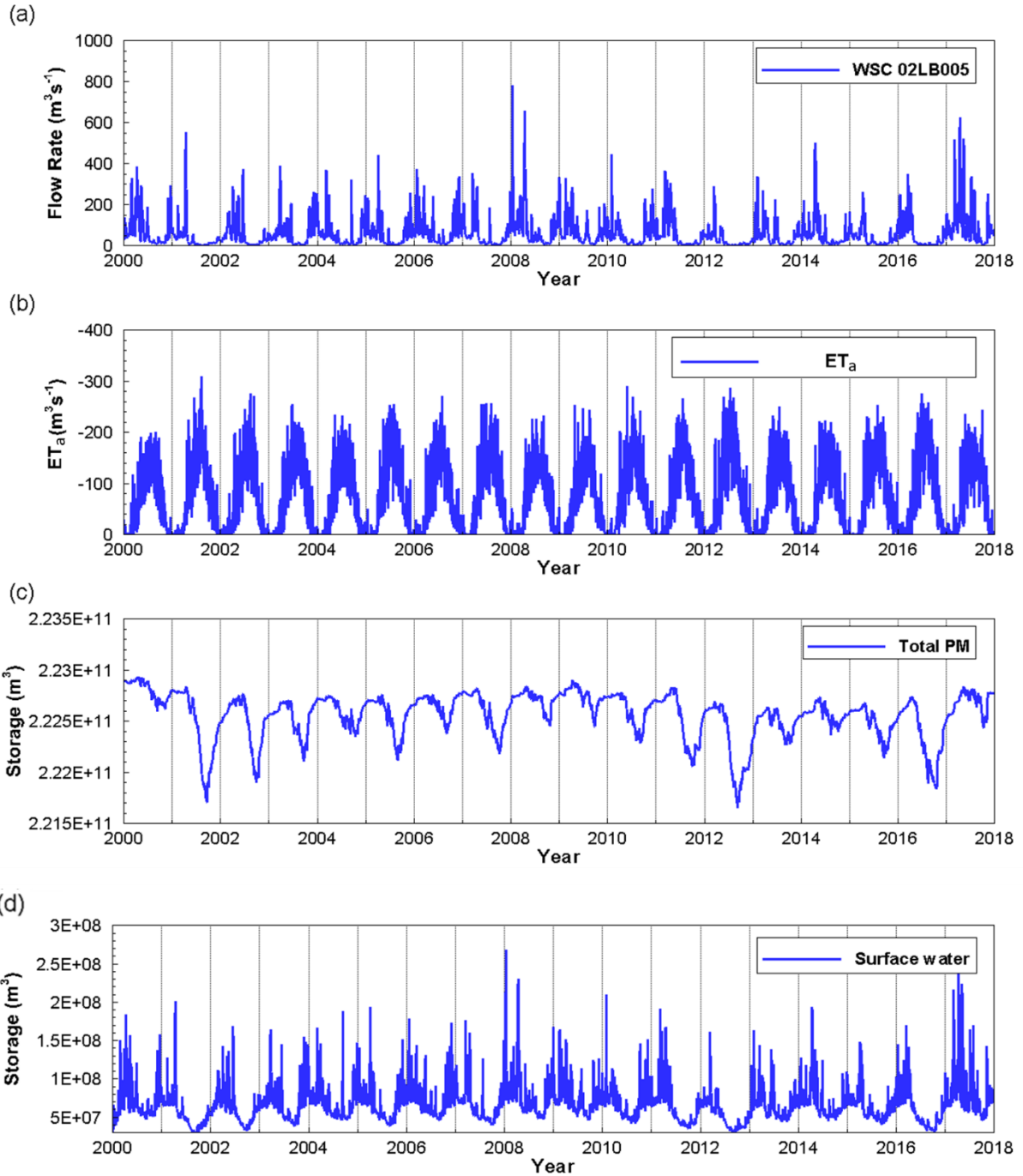
306

307 **Figure 5: Simulated vs. observed surface water flow rates at the nine Water Survey of Canada (WSC) flow gauges**
 308 **incorporated into the model calibration process, along with Nash-Sutcliffe Model Efficiency (NSE) and Percent Bias (PBias**
 309 **in %) performance metrics. Note that not all gauges have a full data record over the 18-year simulation interval.**

310 **Table 1. For the 10 monitoring well locations, observed vs. simulated average groundwater head, and root mean square**
 311 **error between daily temporal resolution observed and simulated head, over the 2000 – 2017 simulation interval.**

Well	Observed Average Head (mASL)	Simulated Average Head (mASL)	RMSE (m)
95	48.2	62.0	13.8
96	99.1	99.1	0.8
97	84.9	86.9	2.1
268	72.4	72.3	0.5
269	68.4	70.9	2.7
350	111.3	109.5	2.1
363	57.4	61.6	4.2
364	43.2	50.3	7.2
378	74.7	77.0	2.4
379	89.4	87.4	1.9

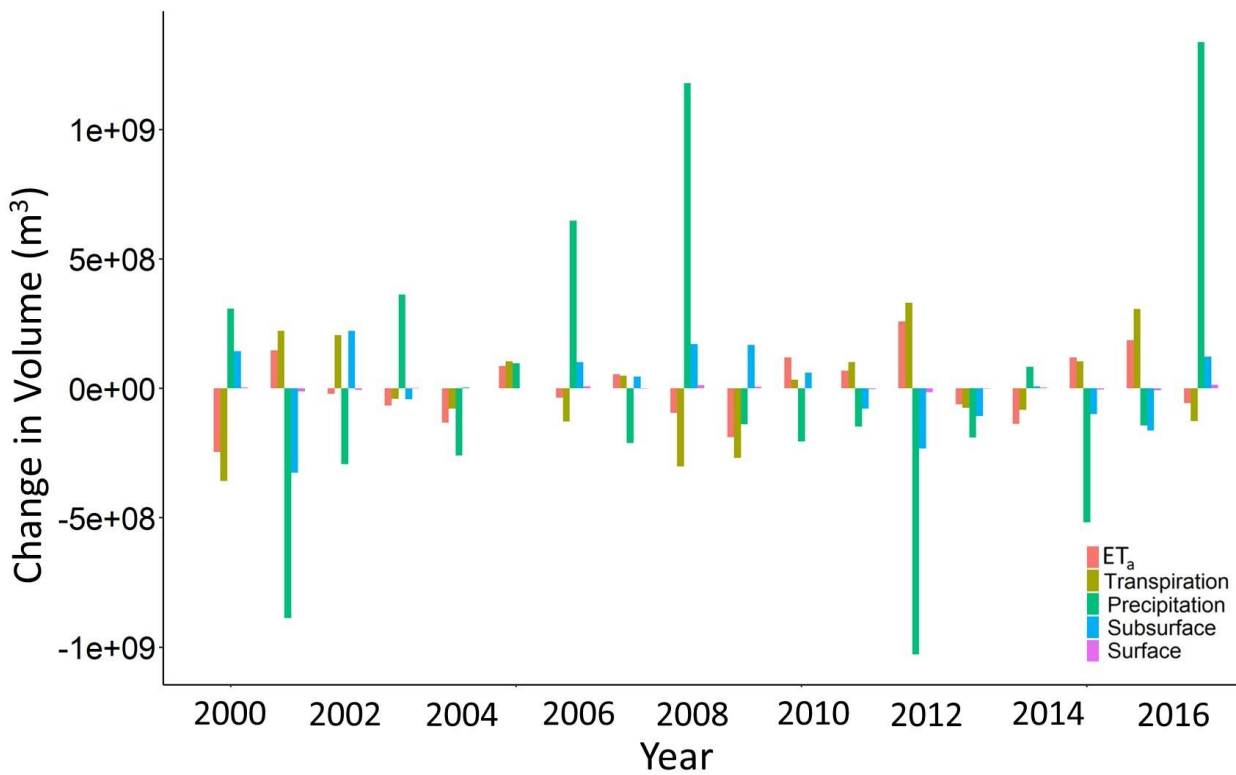
312



313
 314 **Figure 6: Time series outputs from the South Nation watershed HydroGeoSphere (HGS) simulation over the**
 315 **2000-to-2017-time interval. (a) stream flow at the furthest downstream hydrometric station, (b) watershed**
 316 **evapotranspiration, (c) watershed subsurface water storage, and (d) watershed land surface water storage.**

317 The HGS output was generated at variable time steps that were each no larger than 1 day, and then aggregated to
 318 yearly values for use in the ecosystem services assessment (Table A1). Annual deviations from the long term mean,
 319 for ET_a , transpiration, total precipitation, and surface and subsurface water storage, are presented in Fig. 7. In the

320 context of subsequent analysis and discussion, it should be noted that the drought year of 2012 exhibits the highest
 321 ET_a and transpiration, lowest precipitation, and largest relative drops in both subsurface and surface water storage.



322
 323 **Figure 7: Annual deviation from the long term (2000-2017) mean evapotranspiration (ET_a), transpiration,**
 324 **precipitation, and subsurface and surface water storages.**

325 **3.2 Valuation of ecosystem services, and average and marginal water productivity**

326 **Table 2: Land use types and unit values of ecosystem services for the SNW.**

Land Use	Area (hectare)	Unit value (\$/hectare/year)
Water	1,299	165
Urban	25,734	1,177
Wetlands	16,709	71,273
Grasslands	76,961	4,152
Croplands	154,810	1,666
Forest	107,470	4,993

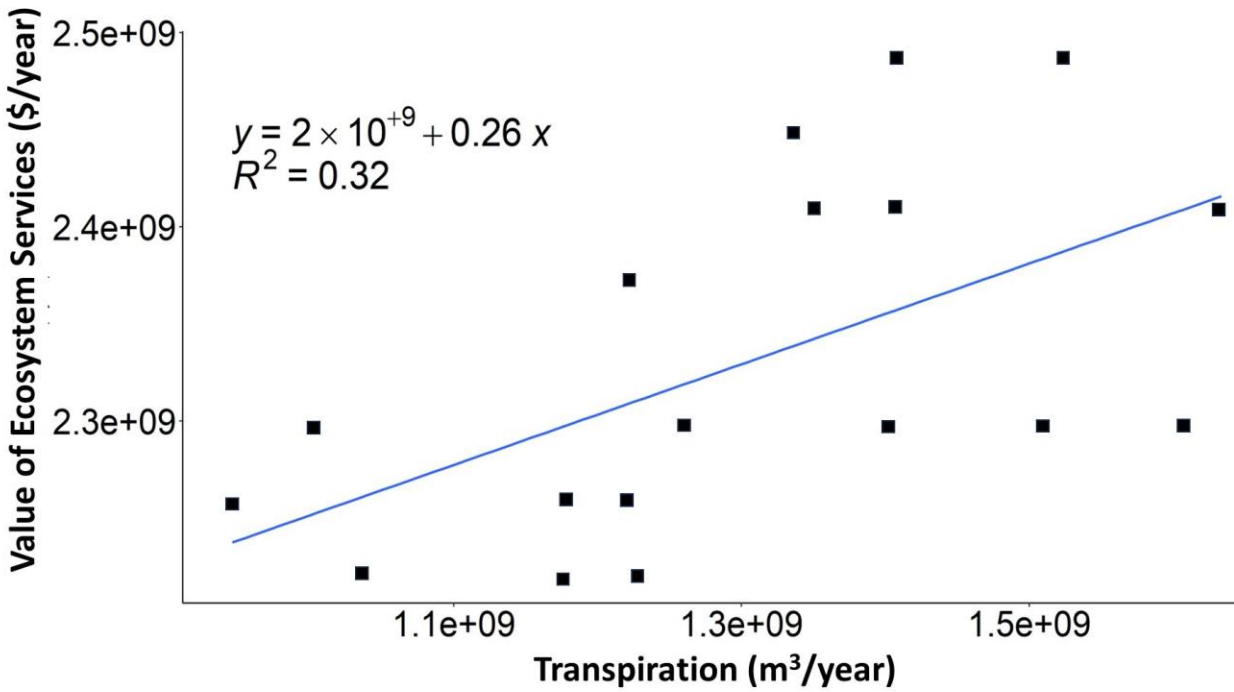
327

328 Using unit values for the major land use types in the SNW (Table 2) and land use area, total value of the 13 ecosystem
 329 services under consideration is \$2.33 billion per year (in CAD 2022) prior to further annual modifications based on
 330 the vegetation indicator (Eq. 1). The estimates for average product of water are point estimates based on the value of
 331 ecosystem services and productive green water volume (i.e., transpiration) for the corresponding year. Annual NPP
 332 data (rescaled between 0 and 1), ES values, transpiration volume, and average water product in the SNW are given in
 333 Table 3.

334 **Table 3: Mean Net Primary Production (NPP), ecosystem services (ES) values, transpiration volume, and**
 335 **average product of water for the SNW over the 18-year study interval.**

Year	Mean NPP	ES Value (x10 ⁹ \$/year)	Transpiration (x10 ⁹ m ³)	Average product of water (\$/m ³)
2000	0.59	2.26	0.95	2.39
2001	0.65	2.49	1.53	1.63
2002	0.6	2.30	1.51	1.52
2003	0.6	2.30	1.26	1.82
2004	0.62	2.37	1.22	1.94
2005	0.63	2.41	1.41	1.71
2006	0.58	2.22	1.18	1.89
2007	0.63	2.41	1.35	1.78
2008	0.6	2.30	1.00	2.29
2009	0.58	2.22	1.03	2.14
2010	0.64	2.45	1.34	1.83
2011	0.6	2.30	1.40	1.63
2012	0.63	2.41	1.63	1.48
2013	0.58	2.22	1.23	1.81
2014	0.59	2.26	1.22	1.85
2015	0.65	2.49	1.41	1.77
2016	0.6	2.30	1.61	1.43
2017	0.59	2.26	1.18	1.92

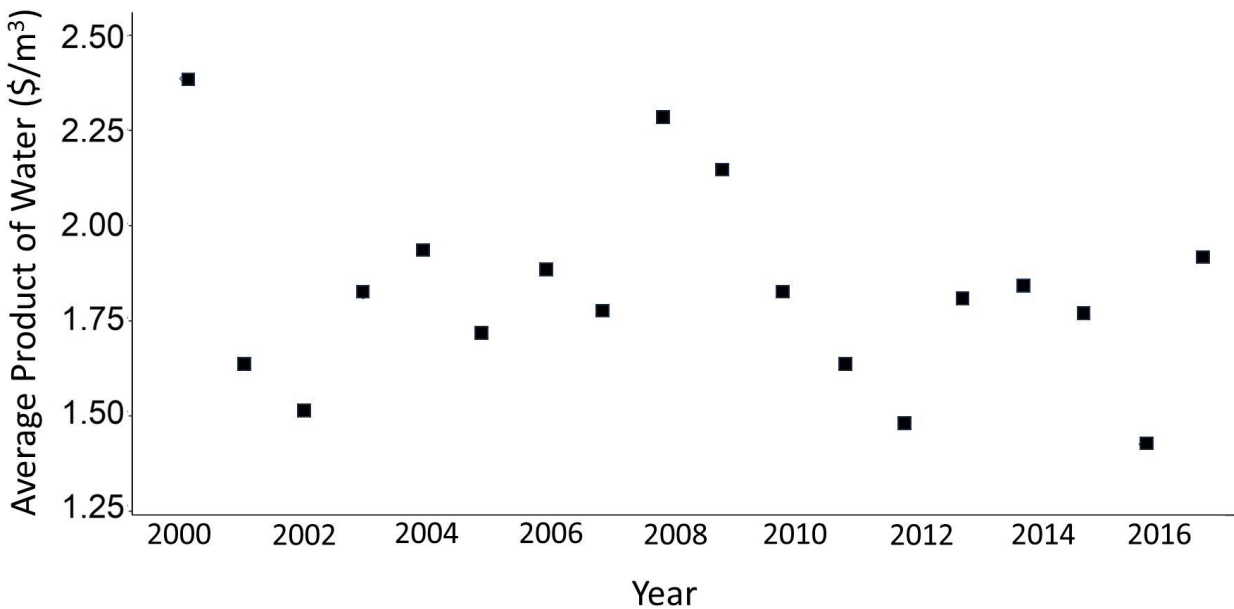
336
 337 For the ecosystem services marginal water productivity, a production function is developed using transpiration and
 338 ecosystem services values for the SNW (Fig. 8) and the slope of the function equates to the marginal productivity of
 339 water, which is \$0.26/m³.



340

341 **Figure 8: Ecosystem services water production function for the SNW.**

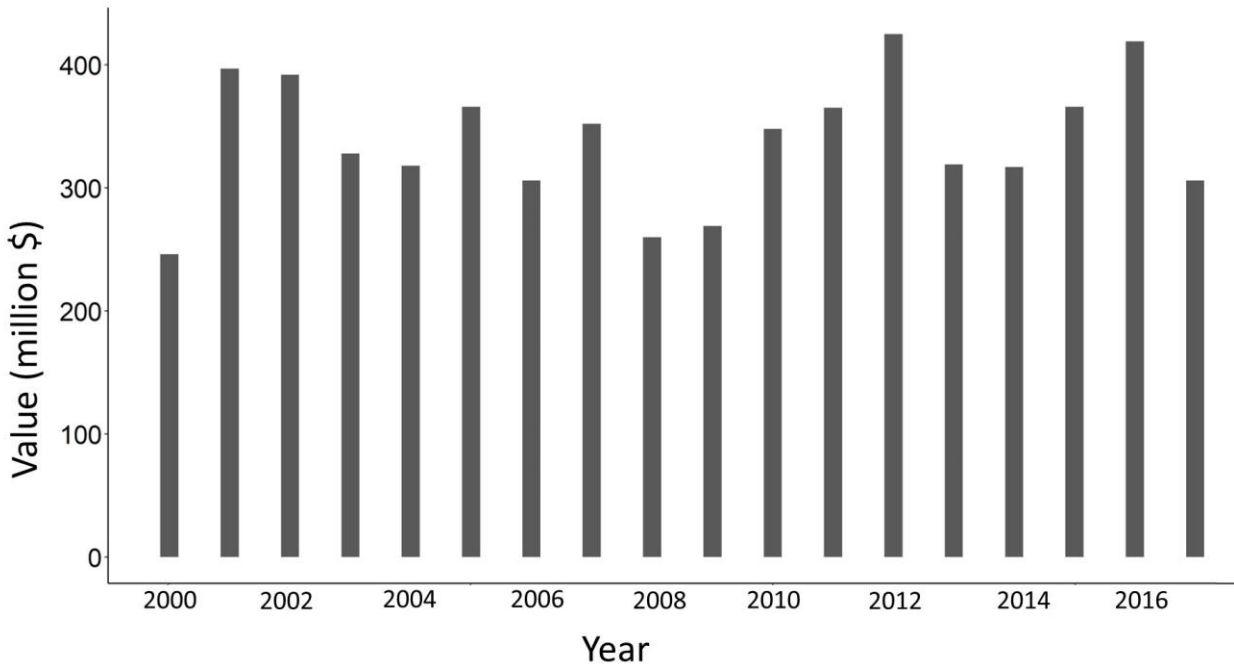
342 To assess the contribution of subsurface water towards ecosystem services, the average ecosystem services water
 343 productivity at the watershed scale is calculated (Table 3). The average product of water over the 18 year study interval
 344 ranges from \$1.43-2.39 per m³ (Fig. 9). During the drier years (2001-2002, 2012 and 2016), the average product of
 345 water declines to local minima. This is because the average product depicts water use efficiency, with the highest
 346 value observed for year 2000 indicating that hydrologic conditions favoured the maximum production of ecosystem
 347 services with the lowest water consumption in that year.



348
 349 **Figure 9: Average annual product of water (Table 3) for ecosystem services in the SNW over the 18-year study**
 350 **period.**

351 **3.3 Valuation of green water**

352 Using the marginal water productivity and transpiration in the SNW, the value of the productive green water (i.e.,
 353 subsurface water) over the study period was calculated (Fig. 10). The annual values range from \$245.9 (year 2000) to
 354 \$424.7 (year 2012) million per year, with an overall average of \$338.83 million. In the SNW, precipitation is the main
 355 driver of the terrestrial hydrologic cycle and low precipitation is the primary indicator of climatological drought. In
 356 general, there is a strong inverse correlation between total annual precipitation and green water value, with an R^2 of
 357 0.45 ($p < 0.0001$).



358

359 **Figure 10: Value of productive green water in the SNW over the 18-year study period.**

360 **4 Discussion**

361 **4.1 Drought Year Hydrologic Behavior**

362 In the study herein, HGS is used to capture the contributions of subsurface water storage to transpiration (i.e.,
 363 productive green water) and quantify its role in sustaining transpiration and subsequent ecosystem services.

364 The annual deviations from the long-term means (Fig. 7) show that ET_a and transpiration are supported by the
 365 subsurface and surface storages during droughts. In the drought period from 2001-2002, an interesting situation arises.

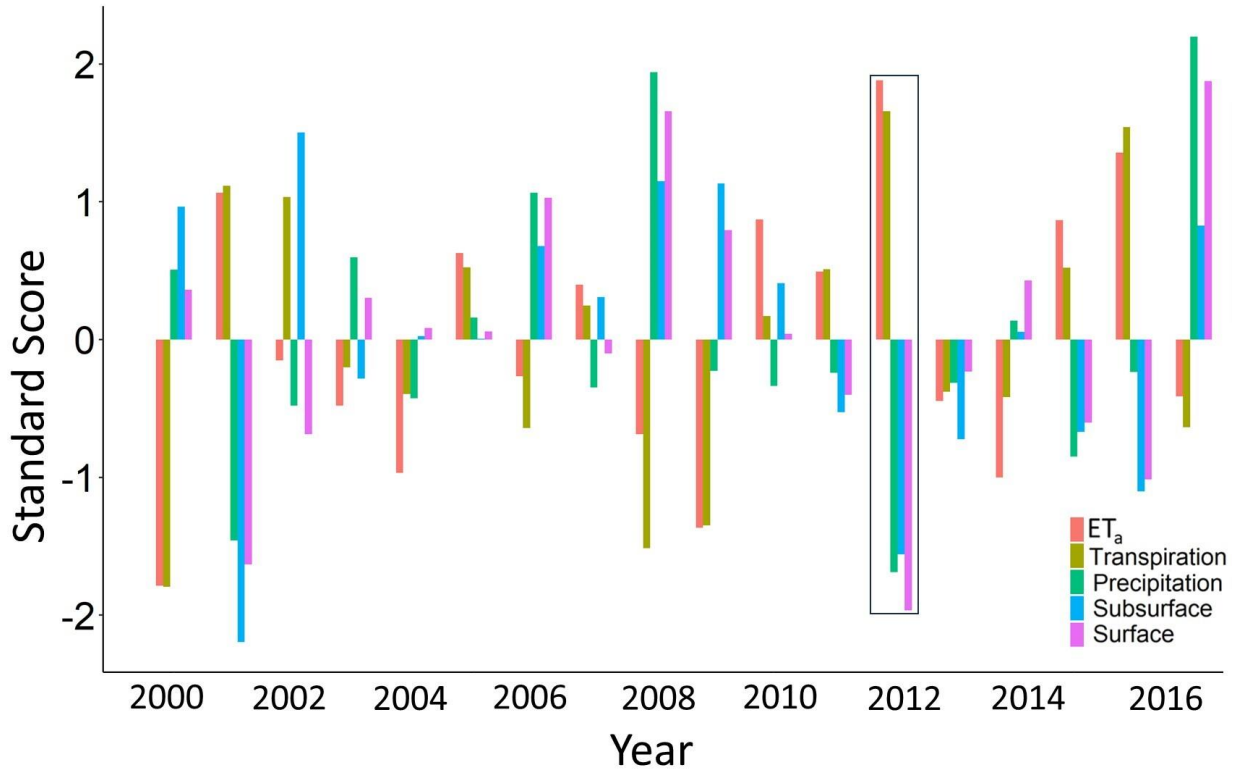
366 In 2001, both ET_a and transpiration exhibit positive values relative to the mean. However, in 2002, despite ET_a being
 367 negative, transpiration remains positive and surpasses the mean value. This deviation can be attributed to the

368 diminished availability of surface water, leading to reduced evaporation and subsequently lower ET_a . Nevertheless,
 369 transpiration continues to exceed the average due to its reliance on subsurface water availability within the SNW. This

370 finding is further supported by previous studies, which suggest that transpiration dominates ET_a during drought years,
 371 while evaporation takes precedence during wet years (Zhang et al., 2019). To further compare the fluctuations in

372 different storage zones on a common scale, the standard scores (that is, the change in a storage/standard deviation) for
 373 each zone are calculated over time (Fig. 11). The standard scores show that ET_a is supported by both surface and

374 subsurface water storages during the dry periods. However, the contribution of subsurface water by volume during
 375 drought is much larger than that of surface water, thus highlighting the important role of subsurface water in supporting
 376 transpiring biota during droughts.



377
 378 **Figure 11: Change in standard scores of water storages/hydrological variables over the 18-year study period.**
 379 **The scores for the 2012 drought year are bordered.**

380 Comparison of years 2001 and 2012 (both with less precipitation than the 18-year mean) shows that the ET_a was less
 381 but outflow was more in 2001 relative to 2012 (Fig. 6(a)). In such case, it is the subsurface water contribution in 2001
 382 that maintained the higher surface water flows, which highlights the important role of antecedent conditions in
 383 regulating low flow response. Nevertheless, the influence of subsurface water on consumptive water use also depends
 384 on the timing of precipitation along with other climatic conditions (e.g., temperature, atmospheric moisture demand,
 385 etc.) in the corresponding years (Zhao et al., 2022). During drought periods, vegetation and atmospheric moisture
 386 demand is often not met, thus resulting in ecosystem stress along with depletion of subsurface and surface water
 387 storages (Zhao et al., 2022). Given the complexities involved with linking transpiration with subsurface water storages,
 388 full characterization of transpiration influences on ecosystem services during droughts has until now received little
 389 attention.

390 The study quantifies subsurface water ecosystem services values, at the scale of a 3830 km² watershed, over a period
391 that encompasses a wide range of climatological conditions. Previous studies (e.g., Loheide, 2008; Su et al., 2022)
392 have estimated groundwater contribution to evapotranspiration by linking water table fluctuation with changes in
393 evapotranspiration. However, over large areas, using water table fluctuation can be complicated by other subsurface
394 water sinks, including deeper groundwater recharge and discharge into surface water receptors. With the HGS
395 approach employed herein, the computed subsurface water evaporation and transpiration, and surface water
396 evaporation, in conjunction with the other hydrologic flow processes depicted in Fig. 2, provides a physical based
397 numeric characterization of water storage contributions to ET_a.

398 The fluctuations in water storages show that, in general and with respect to longer term mean conditions, subsurface
399 water storage repletes when ET_a is negative and depletes when ET_a is positive. In both the 2001 and 2012 drought
400 years, ET_a is relatively high in comparison to the wet years with high precipitation. ET_a in drought years is primarily
401 supported by the drawdown (by volume) in subsurface water storage below the mean level. In general, fluctuations in
402 subsurface water storage across the 18 years are congruent with changes in precipitation, with above-average
403 precipitation aligned with increases in subsurface water storage and vice-versa. In contrast, increased ET_a leads to a
404 reduction in subsurface storage and vice-versa. Over the 18 year study period, the maximum increase in subsurface
405 water storage occurred in the year 2002, immediately following the 2001 drought which had implications far beyond
406 just the SNW (Wheaton et al., 2008). Even though 2002 was a year with less than average precipitation, the drought-
407 impacted subsurface storage conditions led to an antecedent condition across the SNW that was favourable for
408 subsurface water recharge.

409 **4.2 Hydrologic Influences on Ecosystem Services and Economic Valuation**

410 Based on the study herein, fully-integrated groundwater – surface water models, such as HGS, have potential to
411 facilitate better management of watershed scale (approximately 4,000 km²) water resources for ecosystem services
412 endpoints, as well as help determine the role of a range of water resources that sustain green water supply. A water
413 production function was developed using total green water volumes and total values of 13 ecosystem services in the
414 SNW: agricultural services (net benefits from the crops or agricultural products), global climate regulation, air quality,
415 water provision, waste treatment, erosion control, pollination, habitat for biodiversity, natural hazard prevention, pest
416 management, nutrient cycling, landscape aesthetics, and recreational activities. The ecosystem water production

417 function yields a marginal value of \$ 0.26 per m³ of green water devoted to transpiration (Fig. 8). Globally, Lowe et
418 al. (2022) estimated the average marginal product of water specifically for crop production at \$0.083 per m³. While
419 water productivity is greatest when the smallest amount of water is used/consumed, it also produces the smallest value
420 of ecosystem services at this point. Between 2000 and 2017, transpiration in the SNW is highest during the driest
421 years (Zhao et al., 2022). The NPP does not decline during these periods, likely due to enough subsurface water to
422 meet plant demands (e.g., Hosen et al., 2019; Sun et al., 2016). Modeling results presented herein show that the dry
423 meteorological conditions are associated with relatively higher transpiration and ET_a rates, similar to Zhao et al. (2022)
424 and Diao et al. (2021). During dry years, the increase in transpiration is positively correlated with higher NPP, which
425 in turn relates to lower relative ecosystem service water productivity values (Fig. 9).

426 In the SNW, green water use is higher in years with less than average precipitation. Accordingly, green water value
427 was highest, at \$424.7 million (in CAD 2022), for the 2012 drought year (Fig. 10). It is important to note that value
428 of the subsurface water contribution is second highest, at 418.63 million, for 2016, which is also a drought year. Hence,
429 the critical role of subsurface water in sustaining ecosystem services is especially evident during both drought years
430 and more typical climatic conditions.

431 **4.3 Strengths and Limitations of Fully-Integrated GW-SW Models**

432 While the study herein advances the scientific utility of physics-based fully-integrated groundwater–surface water
433 models, it is essential to acknowledge the inherent uncertainty associated with such an analysis, along with factors
434 that could potentially reduce this uncertainty. It is well known that highly parameterized, structurally complex models
435 can have many degrees of freedom, high data requirements, and non-uniqueness challenges (Beven, 2006). However,
436 the parameterization of physics-based models can also be viewed as a strength due to the constraining relationship
437 between physically measurable characteristics and parameter values (Ebel and Loague, 2006). For the SNW, soil and
438 subsurface materials are well characterized and hence the spatial distribution and magnitudes of the associated
439 hydraulic parameters are generally well represented in the HGS model. Incorporating meteorological variability into
440 structurally complex model calibration and performance evaluation can also act to reduce uncertainty (Moeck et al.,
441 2018). Because the SNW simulation extended over an 18-year time frame that included multiple droughts and floods,
442 there is confidence that the model structure and parameterization is suited for a wide spectrum of hydrologic

443 conditions, and that the model can dynamically capture transitions from wet-to-dry and dry-to-wet conditions, which
444 is a critical part of the SNW analysis.

445 Fully-integrated groundwater - surface water models are ideally suited for the type of challenge addressed in the work
446 herein because simpler models lack process representation critical within the problem conceptualization (Ebel and
447 Loague, 2006). This is especially true when considering difficulties associated with quantifying large scale
448 evaporation and transpiration fluxes (Stoy et al., 2019), and groundwater-surface water interactions (Barthel and
449 Banzhaf, 2016). Structurally complex models have been shown to perform better than simple models when simulating
450 evapotranspiration (Ghasemizade et al., 2015) and groundwater recharge (Moeck et al., 2018), and previous work by
451 Hwang et al. (2015) demonstrated the utility of HGS for constraining ET at the watershed scale within the same
452 geographic region as the SNW. Further confidence in the SNW HGS model can be established through comparison
453 with other studies. In terms of overall water balance, results from the study herein compare closely with data compiled
454 as part of regional water management study encompassing the SNW (EOWRMS, 2001). Although the study time
455 frames differ (the EOWRMS (2001) study utilized pre-2000 data), the results are similar, with ETa accounting for
456 approximately 45 % and 62 % of annual precipitation in EOWRMS (2001) and the study herein, respectively. While
457 there is limited previous work investigating the partitioning of ETa into transpiration and evaporation that can be
458 directly compared, it is useful to refer to highly detailed analysis based off Fluxnet data (Pastorello et al., 2020) as
459 reference for transpiration and evaporation partitioning in landcover settings representative of those within the SNW.
460 For example, Xue et al. (2023) reported that transpiration as a percentage of ET ranged (depending on calculation
461 method) from 21-56 % and 39-83 % in Fluxnet data from cropland and mixed forest settings, respectively, whereas
462 the HGS model predicts an aggregate range of 45-65 % across the SNW watershed, which supports the use of HGS
463 transpiration estimates in subsequent ecosystem services valuation.

464 **4.4 Extension to Other Regions**

465 The methodology employed in this study provides a basis for deploying fully-integrated groundwater – surface water
466 models to assess subsurface water contribution to ecosystem services in other regions. However, it must be noted that
467 the results and values used herein are not necessarily transferable to other sites/watersheds. The marginal product of
468 water is a site-specific entity that will be different for other watersheds because both ecosystem services value and
469 transpiration rate will change in response to factors such as land cover, NPP, climate/weather, hydrogeology, and soil

470 properties. Nevertheless, given the ability of fully-integrated models to quantify the dynamic fluctuation in water
471 storages across different compartments, along with the linkage to terrestrial ecosystem services, the approach can be
472 expected to yield reliable results under similar workflow (modelling of water storages and transpiration rates, and
473 valuation of ecosystem services) for other locations/sites/watersheds.

474 **5 Conclusions**

475 This study characterizes and quantifies the important contribution of subsurface water towards sustaining ecosystem
476 services, which, until now has not been comprehensively studied. The prior lack of attention to subsurface water in
477 part relates to the complexities involved with characterizing the dynamic movement of water between subsurface
478 water and surface water storage compartments, and the related supply of green water. In the work herein, focusing on
479 a 3830 km² mixed use watershed, the innovative use of a HGS fully-integrated groundwater – surface water model for
480 water ecosystem services valuation is demonstrated, with the endpoint being monetization of the contributions of
481 subsurface water to green water supply over a period of 18 years (2000-2017). Results show that droughty conditions
482 are a major impetus for increased green water use. The maximum annual productive green water value was \$424.7
483 million (CAD 2022) during the 2012 drought year, while the 18-year average was \$338.83 million. Similarly, in other
484 dry years (i.e., 2001-2002 and 2016), there was a discernible rise in the green water use. Conversely, the results show
485 a notable decrease in the green water use during years characterized by higher precipitation, as exemplified in the year
486 2000 where green water provided \$245.9 million in ecosystem services value. Hence, the study emphasizes the key
487 role of subsurface water in supplying green water and sustaining ecosystem services during critical periods when the
488 watershed is under meteorological drought.

489 Surface water ecosystem services are frequently valued in the literature, whereas the valuation of subsurface water
490 reserves and flows receives considerably less attention. Valuing groundwater resources can provide watershed
491 stewards incentives they can use to support land use management practices that influence flood damages, drought
492 impacts, drinking water quality/quantity, and ecological functions in surface water systems, for instance. The
493 valuation approach provided herein, using integrated numerical hydrogeological models, provides a rigorous
494 standardized means to provision value to ecosystem services associated with all components of the hydrological cycle.
495 This approach offers a template for standardizing water valuation in ecosystem service markets and could guide the
496 integration of water ecosystem service payments across diverse jurisdictions.

497 **Author contribution**

498 Tariq Aziz contributed to concept development, methodology, formal analysis, investigation, modeling, and writing
499 the original draft.

500 Steven K. Frey contributed to concept development, methodology, data curation, HGS modeling, project
501 administration, and reviewing and editing the manuscript.

502 David R. Lapen contributed to methodology development, reviewing and editing the manuscript, and project
503 administration.

504 Susan Preston contributed to methodology development, reviewing and editing the manuscript, and project
505 administration.

506 Hazen A. J. Russell contributed to hydrogeologic characterization, and with reviewing and editing the manuscript.

507 Omar Khader contributed to data curation, HGS model development, and formal analysis.

508 Andre R. Erler contributed to data curation and reviewing the manuscript.

509 Edward A. Sudicky contributed to project administration and reviewing the manuscript.

510 **Declaration of interest**

511 The authors declare that they have no known competing financial interests or personal relationships that could have
512 appeared to influence the work reported in this paper.

513 **References**

514 Agriculture and Agri-Food Canada: Annual Space-Based Crop Inventory for Canada, 2017, Agroclimate, Geomatics
515 and Earth Observation Division, Science and Technology Branch, 2017.

516 Allen, R. G., Pereira, L. S., Raes, D., and Smith, M.: Crop evapotranspiration guidelines for computing crop
517 requirements, Rome, 1998.

518 An, S. and Verhoeven, J. T. A.: Wetlands: Ecosystem services, restoration and wise use, Springer, 325 pp.,
519 <https://doi.org/10.1007/978-3-030-14861-4>, 2019.

520 Aquanty: HydroGeoSphere: A three-dimensional numerical model describing fully-integrated subsurface and surface
521 flow and solute transport, Waterloo, 2021.

522 Arnold, J. G., Srinivasan, R., Muttiah, R. S., and Williams, J. R.: Large area hydrologic modeling and assessment part
523 I: Model development, J. Am. Water Resour. Assoc., 34, 73–89, <https://doi.org/10.1111/j.1752-1688.1998.tb05961.x>,
524 1998.

525 Aziz, T.: Changes in land use and ecosystem services values in Pakistan, 1950–2050, Environ. Dev., 35, 13,
526 <https://doi.org/10.1016/j.envdev.2020.100576>, 2021.

527 Aziz, T., Nimubona, A.-D., and Cappellen, P. Van: Comparative Valuation of Three Ecosystem Services in a Canadian
528 Watershed Using Global, Regional, and Local Unit Values, Sustainability, 15, 17,
529 <https://doi.org/10.3390/su151411024>, 2023.

530 Barthel, R. and Banzhaf, S.: Groundwater and Surface Water Interaction at the Regional-scale – A Review with Focus

531 on Regional Integrated Models, *Water Resour. Manag.*, 30, 1–32, <https://doi.org/10.1007/s11269-015-1163-z>, 2016.

532 Berg, S. J. and Sudicky, E. A.: Toward Large-Scale Integrated Surface and Subsurface Modeling, *Groundwater*, 57,
533 1–2, <https://doi.org/10.1111/gwat.12844>, 2019.

534 Beven, K.: A manifesto for the equifinality thesis, *J. Hydrol.*, 320, 18–36,
535 <https://doi.org/10.1016/j.jhydrol.2005.07.007>, 2006.

536 Bolte, J.: Envision integrated modeling platform, 94 pp., 2022.

537 Booth, E. G., Zipper, S. C., Loheide, S. P., and Kucharik, C. J.: Is groundwater recharge always serving us well?
538 Water supply provisioning, crop production, and flood attenuation in conflict in Wisconsin, USA, *Ecosyst. Serv.*, 21,
539 153–165, 2016.

540 Brunner, P. and Simmons, C. T.: HydroGeoSphere: A Fully Integrated, Physically Based Hydrological Model, *Ground*
541 *Water*, 50, 170–176, <https://doi.org/10.1111/j.1745-6584.2011.00882.x>, 2012.

542 Casagrande, E., Recanati, F., Cristina, M., Bevacqua, D., and Meli, P.: Water balance partitioning for ecosystem
543 service assessment. A case study in the Amazon, *Ecol. Indic.*, 121, <https://doi.org/10.1016/j.ecolind.2020.107155>,
544 2021.

545 Chen, X. and Hu, Q.: Groundwater influences on soil moisture and surface evaporation, *J. Hydrol.*, 297, 285–300,
546 <https://doi.org/10.1016/j.jhydrol.2004.04.019>, 2004.

547 Condon, L. E., Atchley, A. L., and Maxwell, R. M.: Evapotranspiration depletes groundwater under warming over the
548 contiguous United States, *Nat. Commun.*, 11, <https://doi.org/10.1038/s41467-020-14688-0>, 2020.

549 Costanza, R., D’Arge, R., De Groot, R., Farber, S., Grasso, M., Hannon, B., Limburg, K., Naeem, S., O’Neill, R. V.,
550 Paruelo, J., Raskin, R. G., Sutton, P., and Van Den Belt, M.: The value of ecosystem services: Putting the issues in
551 perspective, *Ecol. Econ.*, 25, 67–72, [https://doi.org/10.1016/S0921-8009\(98\)00019-6](https://doi.org/10.1016/S0921-8009(98)00019-6), 1998.

552 Cummings, D. I., Gorrell, G., Guilbault, J., Hunter, J. A., Logan, C., Pugin, A. J., Pullan, S. E., Russell, H. A. J., and
553 Sharpe, D. R.: Sequence stratigraphy of a glaciated basin fill, with a focus on esker sedimentation, *Eol. Soc. Am.*
554 *Bull.*, 1478–1496, <https://doi.org/10.1130/B30273.1>, 2011.

555 Decsi, B., Ács, T., Jolánkai, Z., Kardos, M. K., Koncsos, L., Vári, Á., and Kozma, Z.: From simple to complex –
556 Comparing four modelling tools for quantifying hydrologic ecosystem services, *Ecol. Indic.*, 141,
557 <https://doi.org/10.1016/j.ecolind.2022.109143>, 2022.

558 Dennedy-Frank, P. J., Muenich, R. L., Chaubey, I., and Ziv, G.: Comparing two tools for ecosystem service
559 assessments regarding water resources decisions, *J. Environ. Manage.*, 177, 331–340,
560 <https://doi.org/10.1016/j.jenvman.2016.03.012>, 2016.

561 Diao, H., Wang, A., Yang, H., Yuan, F., Guan, D., and Wu, J.: Responses of evapotranspiration to droughts across
562 global forests: A systematic assessment, *Can. J. For. Res.*, 51, 1–9, <https://doi.org/10.1139/cjfr-2019-0436>, 2021.

563 Ebel, B. A. and Loague, K.: Physics-based hydrologic-response simulation: Seeing through the fog of equifinality,
564 *Hydrol. Process.*, 20, 2887–2900, <https://doi.org/10.1002/hyp.6388>, 2006.

565 Endsley, K. A., Zhao, M., Kimball, J., and Deva, S.: Continuity of global MODIS terrestrial primary productivity
566 estimates in the VIIRS era using model-data fusion, *J. Geophys. Res. Biogeosciences*,
567 <https://doi.org/10.22541/essoar.167768101.16068273/v1>, 2023.

568 EOWRMS: Eastern Ontario water resources management study (final report), Ottawa, Ontario, 5–24 pp., 2001.

569 Erler, A. R., Frey, S. K., Khader, O., d’Orgeville, M., Park, Y. J., Hwang, H. T., Lapen, D. R., Richard Peltier, W.,
570 and Sudicky, E. A.: Simulating Climate Change Impacts on Surface Water Resources Within a Lake-Affected Region
571 Using Regional Climate Projections, *Water Resour. Res.*, 55, 130–155, <https://doi.org/10.1029/2018WR024381>,
572 2019.

573 Foster, S. S. D. and Chilton, P. J.: Groundwater: The processes and global significance of aquifer degradation, *Philos.*
574 *Trans. R. Soc. B Biol. Sci.*, 358, 1957–1972, <https://doi.org/10.1098/rstb.2003.1380>, 2003.

575 Frey, S. K., Miller, K., Khader, O., Taylor, A., Morrison, D., Xu, X., Berg, S. J., Sudicky, E. A., and Lapen, D. R.:
576 Evaluating landscape influences on hydrologic behavior with a fully- integrated groundwater – surface water model,
577 *J. Hydrol.*, 602, 1–8, 2021.

578 Ghasemizade, M., Moeck, C., and Schirmer, M.: The effect of model complexity in simulating unsaturated zone flow
579 processes on recharge estimation at varying time scales, *J. Hydrol.*, 529, 1173–1184,
580 <https://doi.org/10.1016/j.jhydrol.2015.09.027>, 2015.

581 Griebler, C. and Avramov, M.: Groundwater ecosystem services: A review, *Freshw. Sci.*, 34, 355–367,
582 <https://doi.org/10.1086/679903>, 2015.

583 Hogg, E. H.: Temporal scaling of moisture and the forest-grassland boundary in western Canada, *Agric. For.*
584 *Meteorol.*, 84, 115–122, [https://doi.org/10.1016/S0168-1923\(96\)02380-5](https://doi.org/10.1016/S0168-1923(96)02380-5), 1997.

585 Honeck, E., Gallagher, L., von Arx, B., Lehmann, A., Wyler, N., Villarrubia, O., Guinaudeau, B., and Schlaepfer, M.
586 A.: Integrating ecosystem services into policymaking – A case study on the use of boundary organizations, *Ecosyst.*
587 *Serv.*, 49, <https://doi.org/10.1016/j.ecoser.2021.101286>, 2021.

588 Hosen, J. D., Aho, K. S., Appling, A. P., Creech, E. C., Fair, J. H., Hall, R. O., Kyzivat, E. D., Lowenthal, R. S., Matt,
589 S., Morrison, J., Sainers, J. E., Shanley, J. B., Weber, L. C., Yoon, B., and Raymond, P. A.: Enhancement of primary
590 production during drought in a temperate watershed is greater in larger rivers than headwater streams, *Limnol.*
591 *Oceanogr.*, 64, 1458–1472, <https://doi.org/10.1002/lno.11127>, 2019.

592 Hwang, H. T., Park, Y. J., Frey, S. K., Berg, S. J., and Sudicky, E. A.: A simple iterative method for estimating
593 evapotranspiration with integrated surface/subsurface flow models, *J. Hydrol.*, 531, 949–959,
594 <https://doi.org/10.1016/j.jhydrol.2015.10.003>, 2015.

595 Jin, Z., Liang, W., Yang, Y., Zhang, W., Yan, J., Chen, X., Li, S., and Mo, X.: Separating Vegetation Greening and
596 Climate Change Controls on Evapotranspiration trend over the Loess Plateau, *Sci. Rep.*, 7, 1–15,
597 <https://doi.org/10.1038/s41598-017-08477-x>, 2017.

598 Kollet, S., Mauro, S., M., M. R., Paniconi, C., Putti, M., Bertoldi, G., Coon, E. T., Cordano, E., Endrizzi, S., Kikinzon,
599 E., Mouche, E., M€ugler, C., Park, Y.-J., Refsgaard, J. C., Stisen, S., and Sudicky, E.: The integrated hydrologic model
600 intercomparison project, IH-MIP2: A second set of benchmark results to diagnose integrated hydrology and feedbacks,
601 *Water Resour. Res.*, 867–890, <https://doi.org/10.1002/2016WR019191>.Received, 2016.

602 Kornelsen, K. C. and Coulibaly, P.: Synthesis review on groundwater discharge to surface water in the Great Lakes
603 Basin, *J. Great Lakes Res.*, 40, 247–256, <https://doi.org/10.1016/j.jglr.2014.03.006>, 2014.

604 L’Ecuyer-Sauvageau, C., Dupras, J., He, J., Auclair, J., Kermagoret, C., and Poder, T. G.: The economic value of

605 Canada's National Capital Green Network, *PLoS One*, 16, 1–29, <https://doi.org/10.1371/journal.pone.0245045>, 2021.

606 Li, Q., Qi, J., Xing, Z., Li, S., Jiang, Y., Danielescu, S., Zhu, H., Wei, X., and Meng, F. R.: An approach for assessing
607 impact of land use and biophysical conditions across landscape on recharge rate and nitrogen loading of groundwater,
608 *Agric. Ecosyst. Environ.*, 196, 114–124, <https://doi.org/10.1016/j.agee.2014.06.028>, 2014.

609 Liang, X., Lettenmaier, D. P., Wood, E. F., and Burges, S. J.: A simple hydrologically based model of land surface
610 water and energy fluxes for general circulation models, *J. Geophys. Res.*, 99, <https://doi.org/10.1029/94jd00483>, 1994.

611 Liu, Y. and El-Kassaby, Y. A.: Evapotranspiration and favorable growing degree-days are key to tree height growth
612 and ecosystem functioning: Meta-Analyses of Pacific Northwest historical data, 1st Annu. IEEE Conf. Control
613 Technol. Appl. CCTA 2017, 2017-Janua, 7–12, <https://doi.org/10.1038/s41598-018-26681-1>, 2017.

614 Liu, Y., Zhou, R., Wen, Z., Khalifa, M., Zheng, C., Ren, H., Zhang, Z., and Wang, Z.: Assessing the impacts of
615 drought on net primary productivity of global land biomes in different climate zones, *Ecol. Indic.*, 130, 108146,
616 <https://doi.org/10.1016/j.ecolind.2021.108146>, 2021.

617 Logan, C., Cummings, D. I., Pullan, S., Pugin, A., Russell, H. A. J., and Sharpe, D. R.: Hydrostratigraphic model of
618 the South Nation watershed region, south-eastern Ontario, Geological Survey of Canada, 17 pp.,
619 <https://doi.org/https://doi.org/10.4095/248203>, 2009.

620 Loheide, S. P.: A method for estimating subdaily evapotranspiration of shallow groundwater using diurnal water table
621 fluctuations, *Ecohydrology*, 1, 59–66, 2008.

622 Lowe, B. H., Zimmer, Y., and Oglethorpe, D. R.: Estimating the economic value of green water as an approach to
623 foster the virtual green-water trade, *Ecol. Indic.*, 136, 108632, <https://doi.org/10.1016/j.ecolind.2022.108632>, 2022.

624 Mammola, S., Cardoso, P., Culver, D. C., Deharveng, L., Ferreira, R. L., Fišer, C., Galassi, D. M. P., Griebler, C.,
625 Halse, S., Humphreys, W. F., Isaia, M., Malard, F., Martinez, A., Moldovan, O. T., Niemiller, M. L., Pavlek, M.,
626 Reboleira, A. S. P. S., Souza-Silva, M., Teeling, E. C., Wynne, J. J., and Zagnajster, M.: Scientists' warning on the
627 conservation of subterranean ecosystems, *Bioscience*, 69, 641–650, <https://doi.org/10.1093/biosci/biz064>, 2019.

628 Maxwell, R. M., Putti, M., Meyerhoff, S., Delfs, J.-O., Ferguson, I. M., Ivanov, V., Jongho Kim, O. K., Stefan J.
629 Kollet, M. K., Lopez, S., Jie Niu, Claudio Paniconi, Y.-J. P., Mantha S. Phanikumar, C. S., Sudicky, E. A., and Sulis,
630 M.: Surface-subsurface model intercomparison: A first set of benchmark results to diagnose integrated hydrology and
631 feedbacks, *Water Resour. Res.*, 1531–1549, <https://doi.org/10.1002/2013WR013725>.Received, 2014.

632 McKenney, D. W., Hutchiinson, M. F., Papadopol, P., Lawrence, K., Pedlar, J., Campbell, K., Milewska, E.,
633 Hopkinson, R. F., Price, D., and Owen, T.: Customized spatial climate models for North America, *Bull. Am. Meteorol.*
634 *Soc.*, 92, 1611–1622, <https://doi.org/10.1175/2011BAMS3132.1>, 2011.

635 Mercado-bettín, D., Salazar, J. F., and Villegas, J. C.: Long-term water balance partitioning explained by physical and
636 ecological characteristics in world river basins, *Ecohydrology*, 12, 1–13,
637 <https://doi.org/https://doi.org/10.1002/eco.2072>, 2019.

638 Millenium Ecosystem Assessment (MEA): *Ecosystems and Human Well-Being: Synthesis*, Island Press, 285 pp.,
639 <https://doi.org/10.1057/9780230625600>, 2005.

640 Moeck, C., von Freyberg, J., and Schirmer, M.: Groundwater recharge predictions in contrasted climate: The effect of
641 model complexity and calibration period on recharge rates, *Environ. Model. Softw.*, 103, 74–89,

642 <https://doi.org/10.1016/j.envsoft.2018.02.005>, 2018.

643 Moriasi, D. N., Arnold, J. G., Van Liew, M. W., Bingner, R. L., Harmel, R. D., and Veith, T. L.: Model evaluation
644 guidelines for systematic quantification of accuracy in watershed simulations, *Trans. ASABE*, 50, 885–900,
645 <https://doi.org/10.13031/2013.23153>, 2007.

646 Mulligan, M.: User guide for the Co\$ting Nature Policy Support System v.2., <https://goo.gl/Grpbnb>, 2015.

647 Muñoz-Sabater, J., Dutra, E., Agustí-Panareda, A., Albergel, C., Arduini, G., Balsamo, G., Boussetta, S., Choulga,
648 M., Harrigan, S., Hersbach, H., Martens, B., Miralles, D. G., Piles, M., Rodríguez-Fernández, N. J., Zsoter, E.,
649 Buontempo, C., and Thépaut, J. N.: ERA5-Land: A state-of-the-art global reanalysis dataset for land applications,
650 *Earth Syst. Sci. Data*, 13, 4349–4383, <https://doi.org/10.5194/essd-13-4349-2021>, 2021.

651 MYD15A2H MODIS/Aqua Leaf Area Index/FPAR 8-Day L4 Global 500m SIN Grid. NASA LP DAAC:
652 Natural Capital Project: InVEST User Guide 3.12.0, 1–7 pp., 2022.

653 Neff, B. P., Day, S. M., Piggott, A. R., and Fuller, L. M.: Base flow in the Great Lakes basin, *U.S. Geol. Surv. Sci.*
654 *Investig. Rep.*, 32, 2005.

655 Ochoa, V. and Urbina-Cardona, N.: Tools for spatially modeling ecosystem services: Publication trends, conceptual
656 reflections and future challenges, *Ecosyst. Serv.*, 26, 155–169, <https://doi.org/10.1016/j.ecoser.2017.06.011>, 2017.

657 Ontario Geological Survey: Surficial Geology of Southern Ontario, Miscellaneous Release--Data 128-REV. Ontario
658 Geological Survey., 1–7 pp., 2010.

659 Ontario Integrated Hydrology Data: [https://geohub.lio.gov.on.ca/maps/mnrf::ontario-integrated-hydrology-oih-](https://geohub.lio.gov.on.ca/maps/mnrf::ontario-integrated-hydrology-oih-data/about)
660 [data/about](https://geohub.lio.gov.on.ca/maps/mnrf::ontario-integrated-hydrology-oih-data/about).

661 Pastorello, G., Trotta, C., Canfora, E., Chu, H., Christianson, D., Cheah, Y. W., Poindexter, C., Chen, J., Elbashandy,
662 A., Humphrey, M., Isaac, P., Polidori, D., Ribeca, A., van Ingen, C., Zhang, L., Amiro, B., Ammann, C., Arain, M.
663 A., Ardö, J., Arkebauer, T., Arndt, S. K., Arriga, N., Aubinet, M., Aurela, M., Baldocchi, D., Barr, A., Beamesderfer,
664 E., Marchesini, L. B., Bergeron, O., Beringer, J., Bernhofer, C., Berveiller, D., Billesbach, D., Black, T. A., Blanken,
665 P. D., Bohrer, G., Boike, J., Bolstad, P. V., Bonal, D., Bonnefond, J. M., Bowling, D. R., Bracho, R., Brodeur, J.,
666 Brümmer, C., Buchmann, N., Burban, B., Burns, S. P., Buysse, P., Cale, P., Cavagna, M., Cellier, P., Chen, S., Chini,
667 I., Christensen, T. R., Cleverly, J., Collalti, A., Consalvo, C., Cook, B. D., Cook, D., Coursolle, C., Cremonese, E.,
668 Curtis, P. S., D’Andrea, E., da Rocha, H., Dai, X., Davis, K. J., De Cinti, B., de Grandcourt, A., De Ligne, A., De
669 Oliveira, R. C., Delpierre, N., Desai, A. R., Di Bella, C. M., di Tommasi, P., Dolman, H., Domingo, F., Dong, G.,
670 Dore, S., Duce, P., Dufrêne, E., Dunn, A., Dušek, J., Eamus, D., Eichelmann, U., ElKhidir, H. A. M., Eugster, W.,
671 Ewenz, C. M., Ewers, B., Famulari, D., Fares, S., Feigenwinter, I., Feitz, A., Fensholt, R., Filippa, G., Fischer, M.,
672 Frank, J., Galvagno, M., Gharun, M., Gianelle, D., et al.: The FLUXNET2015 dataset and the ONEFlux processing
673 pipeline for eddy covariance data, *Sci. Data*, 7, 1–27, <https://doi.org/10.1038/s41597-020-0534-3>, 2020.

674 Qiu, J., Zipper, S. C., Motew, M., Booth, E. G., Kucharik, C. J., and Loheide, S. P.: Nonlinear groundwater influence
675 on biophysical indicators of ecosystem services, *Nat. Sustain.*, 2, 475–483, [https://doi.org/10.1038/s41893-019-0278-](https://doi.org/10.1038/s41893-019-0278-2)
676 [2](https://doi.org/10.1038/s41893-019-0278-2), 2019.

677 Richardson, M. and Kumar, P.: Critical Zone services as environmental assessment criteria in intensively managed
678 landscapes, *Earth’s Futur.*, 5, 617–632, <https://doi.org/10.1002/2016EF000517>, 2017.

679 Schaap, M. G., Leij, F. J., and Van Genuchten, M. T.: Rosetta: A computer program for estimating soil hydraulic
680 parameters with hierarchical pedotransfer functions, *J. Hydrol.*, 251, 163–176, <https://doi.org/10.1016/S0022->
681 1694(01)00466-8, 2001.

682 Schyns, J. F., Hoekstra, A. Y., Booij, M. J., Hogeboom, R. J., and Mekonnen, M. M.: Limits to the world's green
683 water resources for food, feed, fiber, timber, and bioenergy, *Proc. Natl. Acad. Sci. U. S. A.*, 116, 4893–4898,
684 <https://doi.org/10.1073/pnas.1817380116>, 2019.

685 Siebert, S., Burke, J., Faures, J. M., Frenken, K., Hoogeveen, J., Döll, P., and Portmann, F. T.: Groundwater use for
686 irrigation - A global inventory, *Hydrol. Earth Syst. Sci.*, 14, 1863–1880, <https://doi.org/10.5194/hess-14-1863-2010>,
687 2010.

688 SLC: Soil Landscapes of Canada Version 3.2, 2007–2008 pp., 2010.

689 Stoy, P. C., El-Madany, T. S., Fisher, J. B., Gentine, P., Gerken, T., Good, S. P., Klosterhalfen, A., Liu, S., Miralles,
690 D. G., Perez-Priego, O., Rigden, A. J., Skaggs, T. H., Wohlfahrt, G., Anderson, R. G., Coenders-Gerrits, A. M. J.,
691 Jung, M., Maes, W. H., Mammarella, I., Mauder, M., Migliavacca, M., Nelson, J. A., Poyatos, R., Reichstein, M.,
692 Scott, R. L., and Wolf, S.: Reviews and syntheses: Turning the challenges of partitioning ecosystem evaporation and
693 transpiration into opportunities, *Biogeosciences*, 16, 3747–3775, <https://doi.org/10.5194/bg-16-3747-2019>, 2019.

694 Su, Y., Feng, Q., Zhu, G., Wang, Y., and Zhang, Q.: A New Method of Estimating Groundwater Evapotranspiration
695 at Sub-Daily Scale Using Water Table Fluctuations, *Water (Switzerland)*, 14, 1–14,
696 <https://doi.org/10.3390/w14060876>, 2022.

697 Sun, B., Zhao, H., and Wang, X.: Effects of drought on net primary productivity: Roles of temperature, drought
698 intensity, and duration, *Chinese Geogr. Sci.*, 26, 270–282, <https://doi.org/10.1007/s11769-016-0804-3>, 2016.

699 Sun, G., Hallema, D., and Asbjornsen, H.: Ecohydrological processes and ecosystem services in the Anthropocene: a
700 review, *Ecol. Process.*, 6, <https://doi.org/10.1186/s13717-017-0104-6>, 2017.

701 Tan, S., Wang, H., Prentice, I. C., and Yang, K.: Land-surface evapotranspiration derived from a first-principles
702 primary production model, *Environ. Res. Lett.*, 16, <https://doi.org/10.1088/1748-9326/ac29eb>, 2021.

703 Vigerstol, K. L. and Aukema, J. E.: A comparison of tools for modeling freshwater ecosystem services, *J. Environ.*
704 *Manage.*, 92, 2403–2409, <https://doi.org/10.1016/j.jenvman.2011.06.040>, 2011.

705 Villa, F., Bagstad, K., and Balbi, S.: ARIES: Artificial Intelligence for Environment & Sustainability, 2021.

706 Wheaton, E., Kulshreshtha, S., Wittrock, V., and Koshida, G.: Dry times: Hard lessons from the Canadian drought of
707 2001 and 2002, *Can. Geogr.*, 52, 241–262, <https://doi.org/10.1111/j.1541-0064.2008.00211.x>, 2008.

708 Xu, C., Li, Y., Hu, J., Yang, X., Sheng, S., and Liu, M.: Evaluating the difference between the normalized difference
709 vegetation index and net primary productivity as the indicators of vegetation vigor assessment at landscape scale,
710 *Environ. Monit. Assess.*, 184, 1275–1286, <https://doi.org/10.1007/s10661-011-2039-1>, 2012.

711 Xu, S., Frey, S. K., Erler, A. R., Khader, O., Berg, S. J., Hwang, H. T., Callaghan, M. V., Davison, J. H., and Sudicky,
712 E. A.: Investigating groundwater-lake interactions in the Laurentian Great Lakes with a fully-integrated surface water-
713 groundwater model, *J. Hydrol.*, 594, 125911, <https://doi.org/10.1016/j.jhydrol.2020.125911>, 2021.

714 Xu, Y. and Xiao, F.: Assessing Changes in the Value of Forest Ecosystem Services in Response to Climate Change
715 in China, *Sustain.*, 14, <https://doi.org/10.3390/su14084773>, 2022.

716 Xue, K., Song, L., Xu, Y., Liu, S., Zhao, G., Tao, S., Magliulo, E., Manco, A., Liddell, M., Wohlfahrt, G., Varlagin,
717 A., Montagnani, L., Woodgate, W., Loubet, B., and Zhao, L.: Estimating ecosystem evaporation and transpiration
718 using a soil moisture coupled two-source energy balance model across FLUXNET sites, *Agric. For. Meteorol.*, 337,
719 1–7, <https://doi.org/10.1016/j.agrformet.2023.109513>, 2023.

720 Yang, H., Luo, P., Wang, J., Mou, C., Mo, L., Wang, Z., Fu, Y., Lin, H., Yang, Y., and Bhatta, L. D.: Ecosystem
721 evapotranspiration as a response to climate and vegetation coverage changes in Northwest Yunnan, China, *PLoS One*,
722 10, 1–17, <https://doi.org/10.1371/journal.pone.0134795>, 2015.

723 Yang, X. and Liu, J.: Assessment and valuation of groundwater ecosystem services: A case study of Handan City,
724 China, *Water (Switzerland)*, 12, <https://doi.org/10.3390/w12051455>, 2020.

725 Yu, S., Miao, C., Song, H., Huang, Y., and Chen, W.: Efficiency of nitrogen and phosphorus removal by six
726 macrophytes from eutrophic water Efficiency of nitrogen and phosphorus removal by six macrophytes from eutrophic
727 water, *Int. J. Phytoremediation*, 21, 643–651, <https://doi.org/10.1080/15226514.2018.1556582>, 2019.

728 Zhang, T., Xu, M., Zhang, Y., Zhao, T., An, T., Li, Y., Sun, Y., Chen, N., Zhao, T., Zhu, J., and Yu, G.: Grazing-
729 induced increases in soil moisture maintain higher productivity during droughts in alpine meadows on the Tibetan
730 Plateau, *Agric. For. Meteorol.*, 269–270, 249–256, <https://doi.org/10.1016/j.agrformet.2019.02.022>, 2019.

731 Zhao, M., Aa, G., Liu, Y., and Konings, A.: Evapotranspiration frequently increases during droughts, *Nat. Clim.*
732 *Chang.*, 12, 1024–1030, <https://doi.org/https://doi.org/10.1038/s41558-022-01505-3>, 2022.

733 Zisopoulou, K., Zisopoulos, D., and Panagoulia, D.: Water Economics: An In-Depth Analysis of the Connection of
734 Blue Water with Some Primary Level Aspects of Economic Theory I, *Water (Switzerland)*, 14,
735 <https://doi.org/10.3390/w14010103>, 2022.

736

737 **Appendix**

738 The annual outputs (ET_a , surface water, subsurface water, precipitation and outflow) from the HGS model are given
739 in Table A1.

Table A1: HGS outputs from the SNW simulation

Year	ET_a (m³)	Surface water (m³)	Subsurface water (m³)	Precipitati on (m³)	Outflo w (m³)	Surfac e evapor ation (m³)	Subsur face evapor ation (m³)	Subsurf ace transpir ation (m³)
2000	2,085,53 4,445	69,424,628	222,709,069,4 60	4,199,527, 096	2,513,0 14,025	75,020, 473	184,37 4,990	945,999, 818
2001	2,477,00 4,097	54,513,422	222,240,461,9 50	3,003,497, 233	1,229,1 79,146	49,049, 150	193,68 4,126	1,525,26 3,969
2002	2,309,98 4,877	61,588,887	222,788,771,4 12	3,598,706, 939	1,676,3 67,040	49,496, 381	137,24 6,184	150,943 1,700
2003	2,264,69 6,091	68,998,342	222,524,086,3 05	4,253,877, 105	2,171,6 28,188	63,041, 934	155,34 5,628	1,263,07 3,935
2004	2,197,97 4,479	67,358,376	222,569,571,6 66	3,631,932, 688	1,789,0 88,452	56,472, 059	186,21 7,551	1,224,54 5,264
2005	2,416,95 8,064	67,153,617	222,566,818,8 92	3,988,298, 138	1,933,7 41,551	62,293, 999	203,74 5,742	1407,71 8,083
2006	2,293,95 0,204	74,422,486	222,666,754,3 61	4,538,849, 536	2,510,0 31,879	73,310, 604	176,40 6,194	1,175,39 0,417
2007	2,385,26 0,383	65,967,543	222,611,557,1 49	3,679,748, 277	1,804,6 65,208	55,442, 956	193,05 4,015	1,352,24 7,667
2008	2,236,13 9,918	79,130,070	222,736,726,6 08	5,070,858, 236	3,028,1 06,623	63,243, 999	153,50 5,172	1,001,91 2,242
2009	2,142,95 6,266	72,673,133	222,733,824,1 27	3,753,041, 839	2,207,7 58,076	74,320, 182	175,80 8,767	1,034,71 8,786
2010	2,450,48 0,102	67,043,193	222,626,541,1 97	3,686,832, 140	1,818,1 34,266	78,166, 506	204,92 8,373	1,337,19 4,629
2011	2,398,27 5,129	63,710,702	222,487,837,8 13	3,743,641, 761	1,860,0 99,758	56,432, 877	170,45 9,783	1,404,94 3,119

2012	2,589,09	52,013,667	222,334,569,7	2,864,258,	951,529	58,974,	223,34	1,633,46
	4,745		69	811	,742	276	8,145	5,101
2013	2,269,22	64,978,113	222,458,625,7	3,700,833,	1,683,2	67,961,	205,25	1,227,71
	8,484		10	331	28,427	698	3,614	2,022
2014	2,193,04	69,944,514	222,574,462,5	3,974,971,	2,057,6	67,115,	170,74	1,220,17
	1,030		08	693	32,005	318	0,982	9,455
2015	2,449,70	62,201,787	222,466,595,8	3,374,434,	1,324,1	64,640,	227,93	1,407,05
	2,370		16	139	57,589	268	7,634	2,424
2016	2,516,78	59,120,794	222,402,665,8	3,747,4429	1,659,8	53,448,	220,31	1,610,08
	0,613		68	09	95,299	526	3,313	7,162
2017	2,273,90	80,775,412	222,688,809,4	5,228,987,	3,333,1	77,841,	192,36	1,176,49
	3,311		35	865	68,400	432	9,477	7,385

The SNW has approximately 110 m of vertical relief from its highest point in the southwest corner to its outlet at the Ottawa

745 River at its northern edge (Fig. A1).

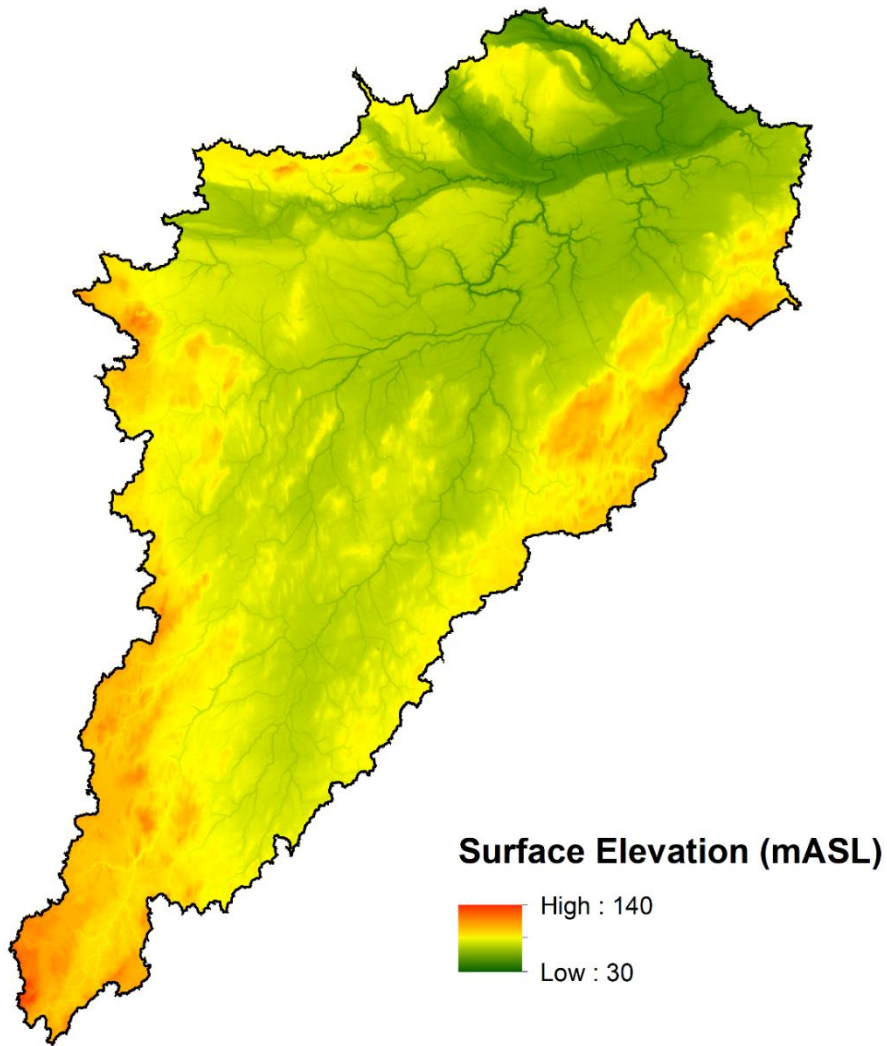
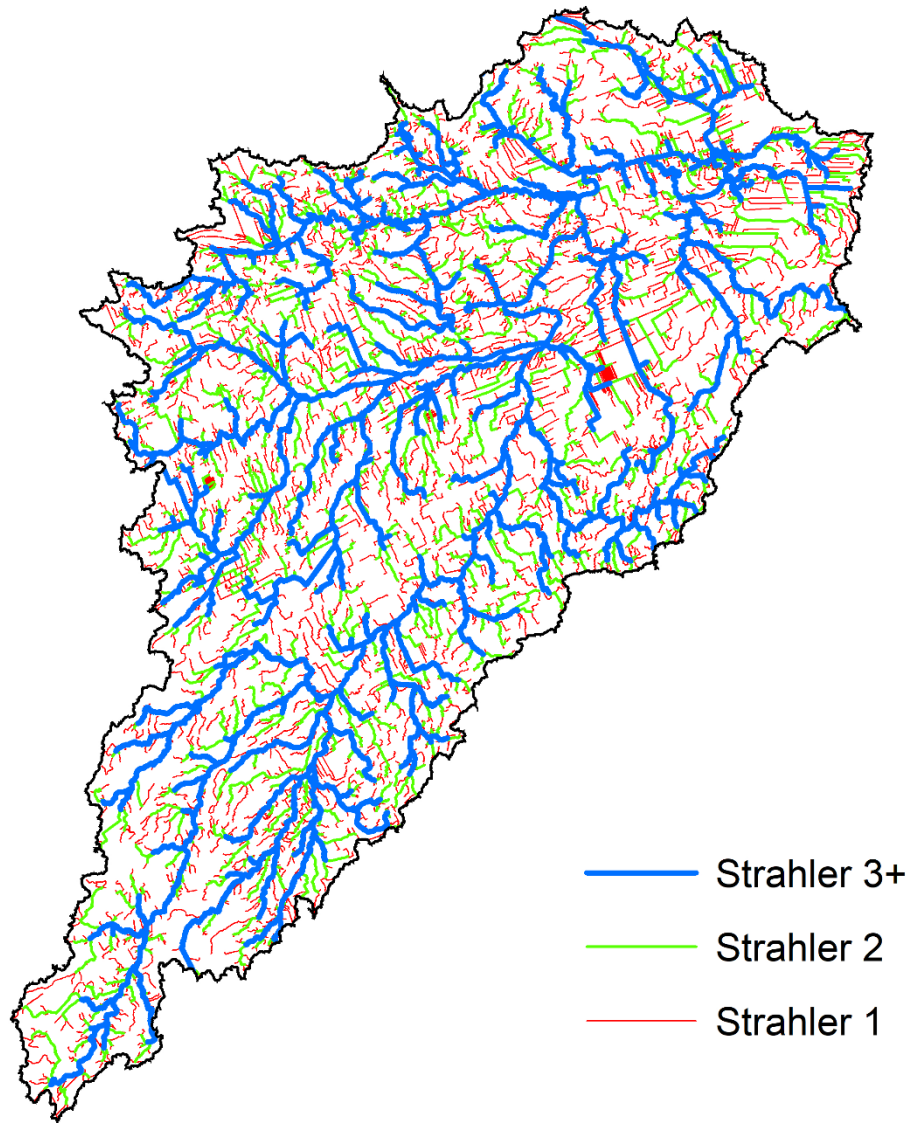


Figure A1: Land surface elevation of the SNW (Ontario Integrated Hydrology Data).



750

Figure A2. Stream network distribution across the South Nation watershed, consisting of 1606 km of Strahler 3+ streams, 1548 km of Strahler 2 streams, and 3335 km of Strahler 1 streams (Ontario Ministry of Natural Resources and Forestry 2013).

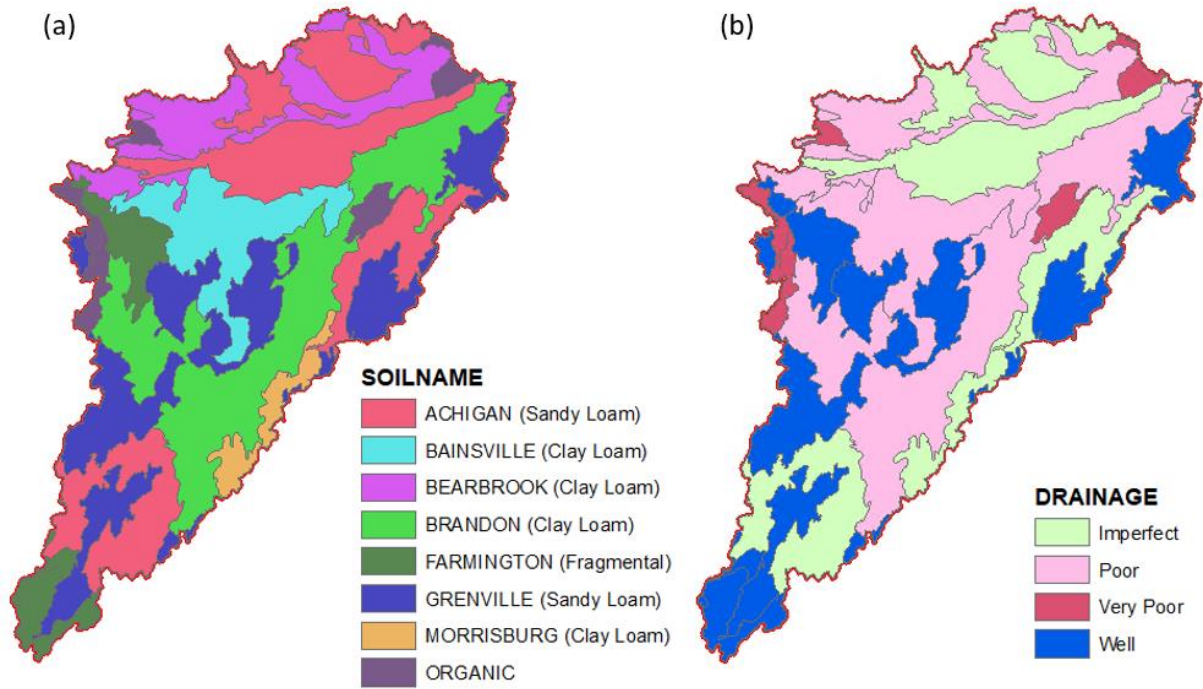
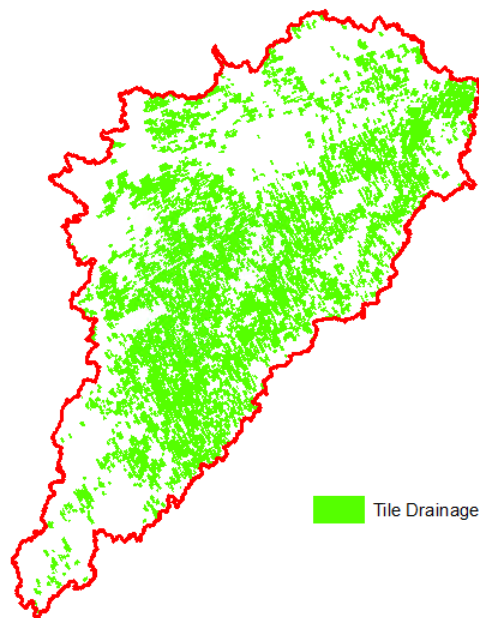


Figure A3. (a) Soil distribution, and (b) soil drainage status across the South Nation watershed (SLC, 2010) .



755

Figure A4. Tile drainage distribution across the South Nation watershed (data provided by the South Nation Conservation Authority).

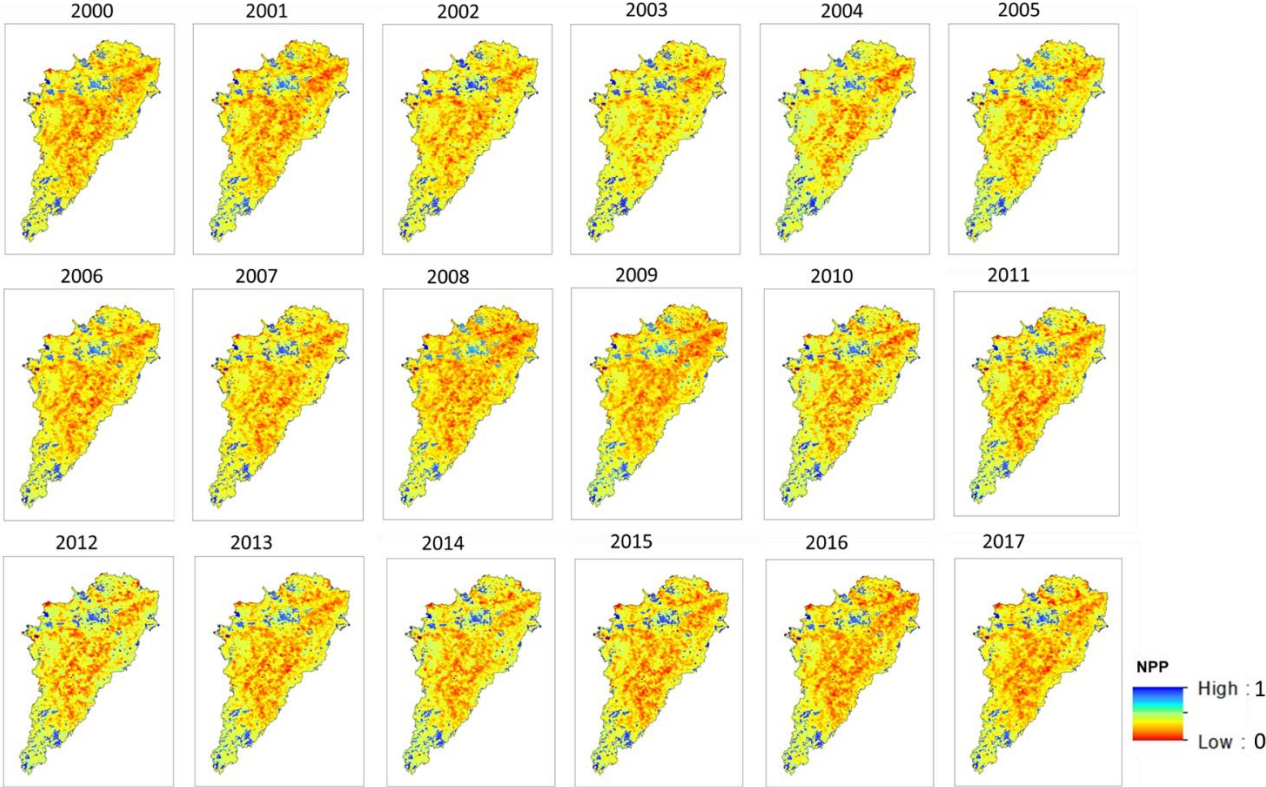


Figure A5: Net Primary Productivity (NPP) data for SNW (based on MODIS data (Endsley et al., 2023))